CHAPTER 4

RESULTS AND DISCUSSION

This chapter provides the results and discussions of the research work as per the set objectives as mentioned in chapter 1. The chapter includes three sections, in ***section 4.1****, a development of a spectrum-integrated thermal and electrical modeling of the PV module is discussed. The analysis of the obtained results and their attributes are detailed in this section.* ***Section 4.2*** *discusses the effect of soiling on the performance of the PV module. The correlation between the soiling of the PV module and environmental parameters based on seasonality is obtained. The electrical performance of PV modules due to soiling is also discussed in this section. Further,* ***section 4.3*** *presents validation of the developed model using statistical errors. The seasonal energy yield analysis is carried out for the PV module technologies under clean and soiled conditions.*

4.1 Development of the spectrum-integrated electrical-thermal model

As discussed in section 3.1.1 of chapter 3, the instantaneous solar spectrum during different time of a day in a season is generated. For instance, the instantaneous solar spectrum generated for the varying environmental parameters for the pre-monsoon season is shown in Figure 4.1(a), and at an instant of local time (12:00) for various seasons is depicted in Figure 4.1(b). The maximum intensity of spectral irradiance is observed between 11:00-12:00 local time, as it is the solar noon (low AM value) period during the pre-monsoon season. The intensity of spectral irradiance decreases with increasing AM value (which can be observed in the early morning and late evening). The major change in the shape of the solar spectrum for an instant of time occurs in the visible region under changing seasons, as in Figure 4.1(b). The diurnal spectrum is generated for the considered representative day of various seasons, which is then used in the electric-thermal model.

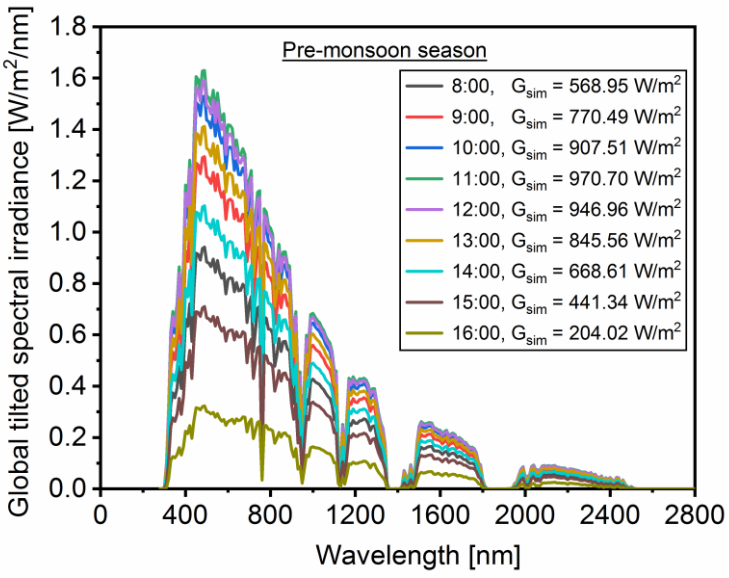

(a)

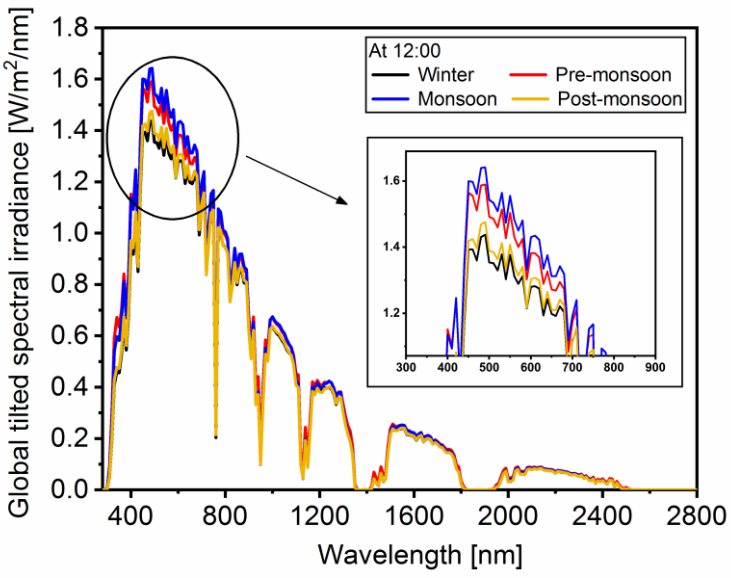

(b)

Figure 4.1 Generated solar spectrum using SMARTS at (a) various time of the day and (b) 12:00 local time during various seasons of the year.

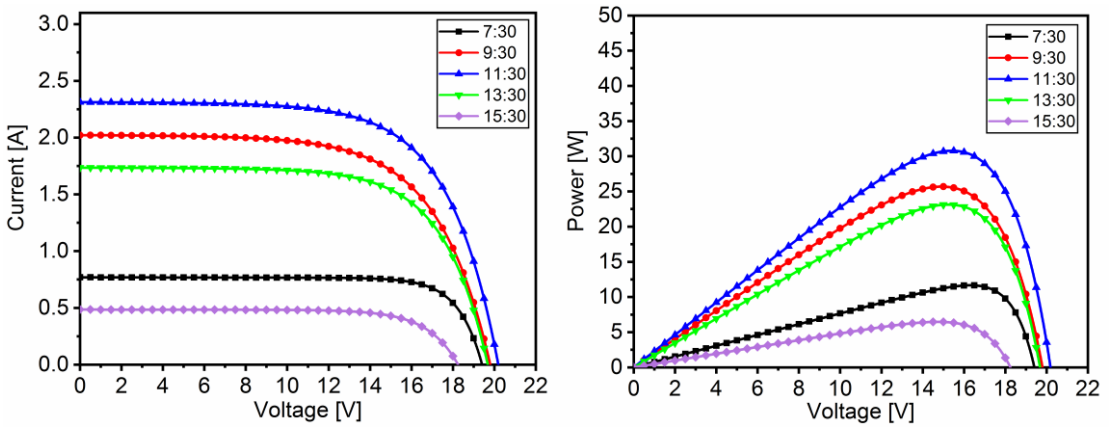

(a) (b)

Figure 4.2 Modeled (a) current-voltage and (b) power-voltage curves of the PV model under the varying solar spectrum.

The developed electrical model generates the electrical parameters of the PV module. Under the varying spectral irradiance (generated from the spectral model as described in section 3.1.1) and cell temperature (generated from the thermal model as described in section 3.1.2), provides the *I-V* and *P-V* characteristics of the PV module. Figure 4.2(a)-(b) show the electrical characteristics of the PV module at a different time of the day simulated for a clear day of the winter season. The power output increase with the rise in the spectral irradiance and reaches the maximum at noon.

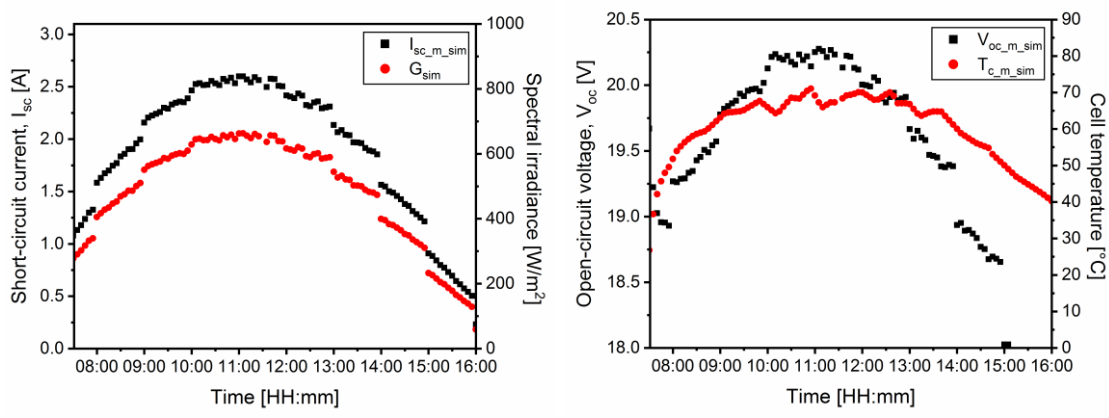

(a) (b)

Figure 4.3 Diurnal variations of (a) short-circuit current, I_{sc} with spectral irradiance, and (b) open-circuit voltage, V_{oc} with cell temperature of the PV module. Subscripts '*m*' depicts m-Si, '*p*' for p-Si, and '*sim*' for simulation.

Figure 4.3(a) depicts the diurnal variation of the simulated short-circuit current (I_{sc}) of the m-Si PV module with varying spectral irradiance (G_{sim}). The I_{sc} value changes proportionally with the varying spectral irradiance. Rise in instantaneous G_{sim} from 609.62 W/m^2 to 620.93 W/m^2 (at T_c of 68°C), the I_{sc} value increases from 2.39 A to 2.44 A, and for the decrease in instantaneous G_{sim} from 638.05 W/m^2 to 616.17 W/m^2 (at T_c of 70°C), the I_{sc} value reduces from 2.50 A to 2.42 A. The variations in I_{sc} also include the effect of cell temperature; however, its impact is comparatively lower than the impact of spectral irradiance. The diurnal change in simulated open-circuit voltage (V_{oc}) of the m-Si PV module with the varying cell temperature (T_c) of the PV module is shown in Figure 4.3(b). The V_{oc} varies inversely proportional to the T_c of the PV module. It is observed that with the instantaneous rise in T_c of the PV module from 64.85°C to 66.10°C (at G_{sim} of 642 W/m^2), the V_{oc} value reduces to 20.21 V to 20.19 V, and with the instantaneous decrease in T_c from 71.04°C to 69.16°C (and their respective G_{sim} of 645.55 W/m^2 to 662.84 W/m^2, respectively), the V_{oc} increase from 20.14 V to 20.25 V.

The effect of the rise in cell temperature on the electrical characteristics of the PV module at constant irradiance is also investigated, as shown in Figure 4.4. The temperature range is considered to be 30°C to 60°C, because the practical cell temperature is mostly in this range for most of seasons for site under study.

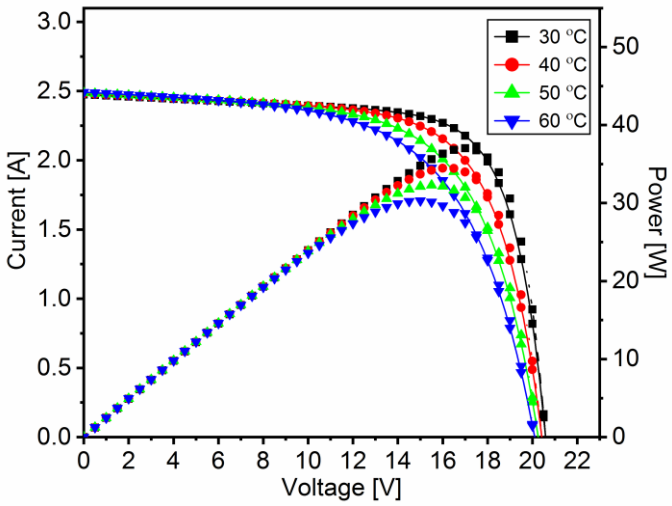

Figure 4.4 Variation in the *I-V* and *P-V* curve of the PV module due to varying cell temperature at constant irradiance of 595 W/m^2.

Table 4.1 Variation of open-circuit voltage, short-circuit current and power output with cell temperature at constant irradiance of 595 W/m^2.

At constant G_{sim} = 595 W/m^2			
Cell temperature T_c (°C)	**Open-circuit voltage V_{oc} (V)**	**Short-circuit current I_{sc} (A)**	**Power P_{max} (W)**
30	20.50	2.475	21.42
40	20.40	2.480	20.33
50	20.20	2.486	19.41
60	20.00	2.492	18.52

It is observed that with the rise in temperature, the V_{oc} decreases and I_{sc} slightly increases as shown in Table 4.1. For 10°C rise in cell temperature with constant spectral irradiance, the relative change in V_{oc} is -0.48%, and I_{sc} is 0.22%. Therefore, the power also decreases as the decrease in V_{oc} was comparatively greater than the increase in I_{sc}. Therefore, the model is observed to work well as per the variations of the input variables and governing equations.

Figure 4.5(a)-(b) shows the distribution of the temperature during the winter season at different layers of the PV module at an instant and also the diurnal temperature variation at points such as the back surface, cell, and glass surface of the PV module. Here, for the average global spectral irradiance of 531.27 W/m^2 and average ambient temperature of 24.68°C during the local time period of 7:30 to 16:00 with 5 minutes interval, it is observed that the temperature is highest in the cell. The back surface and front glass surface of the PV module have a slight difference in temperature. The average cell temperature ($T_{c\_m\_sim}$) is 44.33°C, the average back surface temperature ($T_{b\_m\_sim}$) is 43.01°C, and the average front glass surface temperature ($T_{f\_m\_sim}$) is 43.17°C. The average relative change between the cell temperature and back surface temperature is 0.030 and between the cell temperature and glass surface temperature is 0.026.

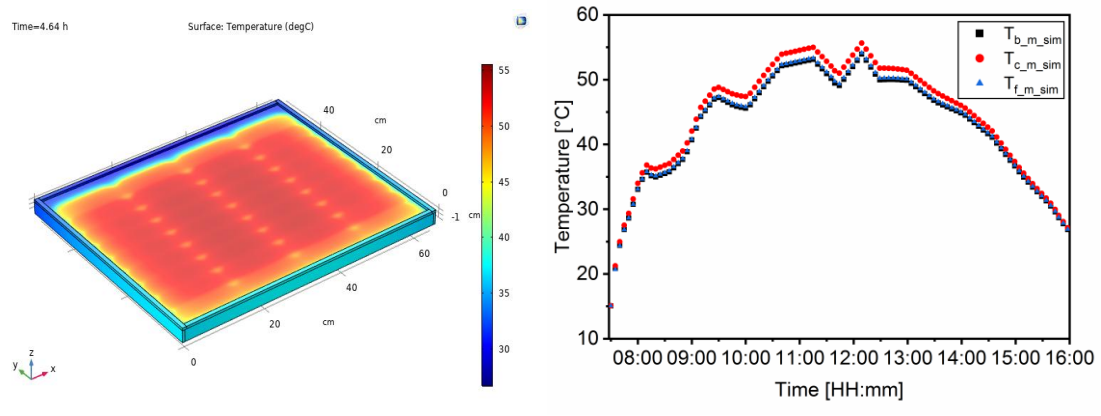

(a) (b)

Figure 4.5 Temperature distributions (a) at an instant and (b) diurnal change in temperature at different layers (back surface, cell, and front glass surface) of the modeled PV module during the winter season.

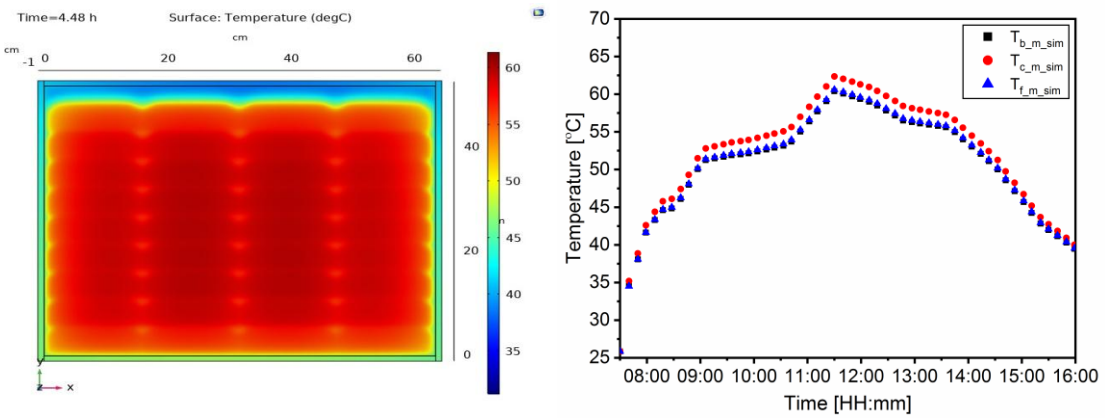

(a) (b)

Figure 4.6 Temperature distributions (a) at an instant and (b) diurnal change in temperature at different layers (back surface, cell, and front glass surface) of the modeled PV module during the pre-monsoon season.

Similarly, the simulated temperature variation during the pre-monsoon season is presented in Figure 4.6. Here, for average global irradiance of 595.1 W/m^2 and T_{amb} of 29.8°C, $T_{c\_m\_sim}$ is 52.3°C, $T_{g\_m\_sim}$ and $T_{b\_m\_sim}$ temperature is 51°C and 50.8°C, respectively. Hence, the electrical parameters are successfully extracted from the electrical model. The developed model, therefore, can generate the power or energy output of the PV module under the transient solar spectrum, cell temperature, and environmental parameters. This spectrum-integrated electrical-thermal model is validated using the experimental results and is discussed in section 4.3. The

experiments are conducted on representative, clear days of different seasons to check the model's flexibility under varying seasons.

4.2 Effect of environmental parameters and soiling on the PV performance

The results in this section aim to analyze the effect of soiling on the optical loss of PV modules. The result evaluates (i) the effectiveness of different cleaning cycles, (ii) the correlations between rain intensity, cleaning effect and artificial cleaning schedules, and (iii) the energy yield of the PV module under soiling. Overall, this work focuses on the PV community's demand for improved model to predict the soiling losses and adequate mitigation solutions.

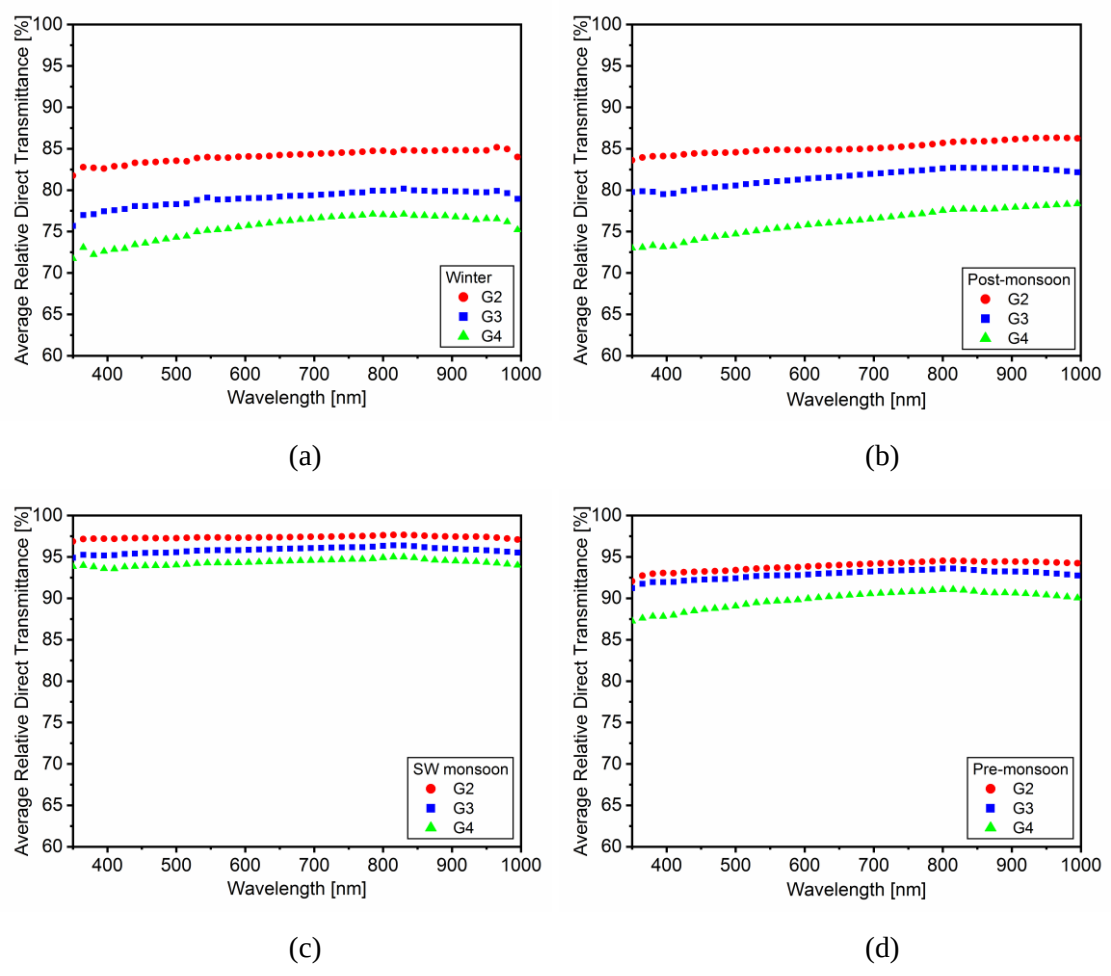

Figure 4.7 Representative relative solar-weighted transmittance of glass coupons with different cleaning cycles due to soiling during (a) winter, (b) post-monsoon, (c) south-west (SW) monsoon, and (d) pre-monsoon seasons.

Following section 3.2 of chapter 3, the variations in the relative direct transmittance of outdoor exposed glass coupons weekly cleaned (G2), monthly cleaned (G3), and never cleaned (G4) for the representative day of the seasons are shown in Figure 4.7(a)-(d). The transmittance of the glass coupons for the different wavelength ranges of the solar spectrum: UV (280-380 nm), visible (380-780 nm), and near-infrared (780-1000 nm) has been measured. During the winter season, a significant change in the solar spectrum is found compared to other seasons. During the south-west (SW) monsoon season, all the glass coupons have resulted minimum variations in the solar spectrum compared to the clean glass, with the least differences for different cleaning cycles. It is also observed that the dust deposition is not constant throughout the year on a single glass coupon and different seasons can affect differently on the various coupons. For some weeks, the transmittance value of the glass coupon G4 which is never cleaned, and G3 which is monthly cleaned, almost overlap during the post-monsoon season, and during winter, G3 showed more shift in the solar spectrum compared to G4. This indicates that the monthly duration may not be sufficient for comparative analysis of dust deposition during winter because of its long dry days between the cleaning schedules. The high PM10 concentration (as in section 3.3) and the non-uniform distribution of dust particles on the area of the glass surface, resulting partial shading and might have resulted in the different transmittance of glass coupons [244].

4.2.1 Relative direct transmittance and transmittance loss of glass coupons

It can be observed that at the initial two weeks after installation, the transmittance of all outdoor installed glass coupons reduces by 8% to 13% compared to the clean glass. This may be because of the electrostatic attraction of charged dust particles towards the clean surface at initial period [185]. During a long dry period of 3 weeks (29^{th} week to 31^{st} week) during the post-monsoon season, G2, G3, and G4 exhibited a drop in transmittance to 79%, 76%, and 74%, respectively. Similarly, it is observed that the transmittance of G4 has dropped to 63% of the G1 after a long dry period of 4 weeks (35^{th} week to 38^{th} week) during the winter season. The maximum drop in transmittance value of G3 and G2 over a year compared to clean glass is around 68% and 71%, respectively. These maximum drops in the transmittance value

of all the glass coupons are obtained during the winter season. A significant drop in the transmittance value of the glass coupons is observed during the winter season. These drops in the transmittance of the glass coupons with different cleaning schedules are affected by the environmental parameter of the location with the seasonal change. The average relative transmittance value of glass coupon with weekly cleaning cycle is 91%, 0.97%, 88%, and 83% during pre-monsoon, SW monsoon, post-monsoon, and winter seasons, respectively. Similarly, this value for glass coupon with monthly cleaning cycle is 90%, 94%, 85%, and 82%, and when left uncleaned is 85%, 93%, 82%, and 76%, during pre-monsoon, SW monsoon, post-monsoon, and winter seasons, respectively.

Figure 4.8 shows the variation in the weekly τ_r of the glass coupons G2, G3, and G4 relative to G1 (clean glass) and also the total rain intensity during the week. The transmittance losses (calculated using equation (3.37)) due to soiling in the various seasons can be ranked in this order: winter > post-monsoon > pre-monsoon > SW monsoon. The maximum average transmittance loss (τ_{loss}) is 24.4% for G4, 18.4% for G3, and 16.6% for G2, all recorded during the winter season. This method utilizes a frequency distribution plot as shown in Figure 4.9 to aggregate and analyze the data in Figure 4.8 for each of the three cleaning cycles. A glass coupon, when cleaned weekly, maintains a high frequency of τ_r above 96%, while for never cleaned, the τ_r can decrease down to 63.6% over the year. Based on the cleaning cycle, the maximum decrease is found in G4, followed by G3 and G2.

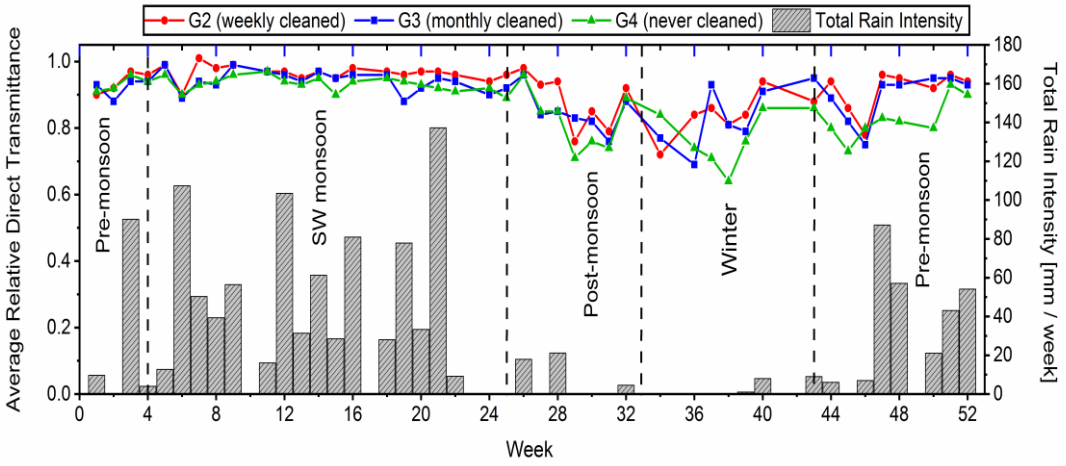

Figure 4.8 The average relative direct transmittance of glass coupons with different cleaning cycles (G2, G3, and G4) and total rainfall intensity in consecutive weeks of the year.

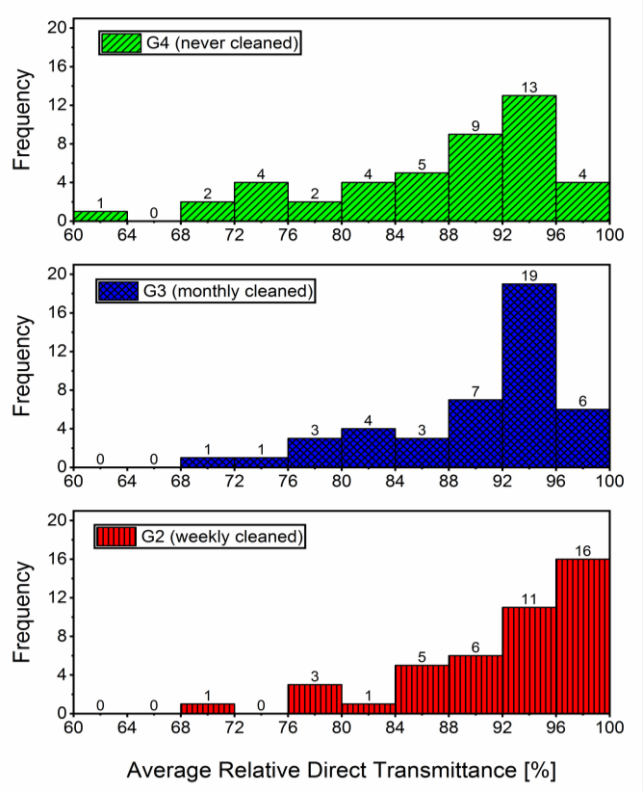

Figure 4.9 Frequency distribution of the average relative direct transmittance of the weekly cleaned, monthly cleaned and never cleaned glass coupons over the year.

It is known that long exposure of glass in the outdoor field uncleaned, reduces the spectral transmittance of the glass coupon. Even with the high occurrence of rainfall, the glass coupons exposed to the outdoor environment undergo optical changes unless cleaned. This may be due to the adhesion of the dust particles on the glass; also, the bird dropping does not wipe out completely during rainfall. The seasonal and annual average τ_{loss}, uncertainty (u), and standard deviation (SD) of all the glass coupons are listed in Table 4.2 depicts the standard deviation and uncertainty calculation (using equations (1.7) and (1.8), respectively). The SD and u for different glass coupons ranges from ±2.2 to ±9.1 and from ±0.7 to ±3.3, respectively. Here, the average relative direct transmittance is the average for measurements taken at three spots of the glass coupon over the wavelength 350-1000 nm. To understand the seasonal net soiling, given the high uncertainty and variability in the data, a statistical t-test analysis is performed. This is described section 4.2.3.

Table 4.2 The seasonal and annual average transmittance loss (τ_{loss} in %), the average seasonal uncertainty (u in %), and seasonal average standard deviation (SD in %) in the average relative direct transmittance (τ_r) of different glass coupons.

Seasons	G2			G3			G4		
	τ_{loss} (%)	u (%)	SD (%)	τ_{loss} (%)	u (%)	SD (%)	τ_{loss} (%)	u (%)	SD (%)
Pre-monsoon	8.5	±1.8	±5.3	9.6	±1.9	±6.2	14.5	±2.7	±6.9
SW monsoon	3.4	±0.9	±2.2	5.8	±0.9	±3.1	6.6	±0.8	±2.3
Post-monsoon	11.9	±2.2	±8.3	15.1	±2.3	±6.2	17.5	±3.4	±8.8
Winter	16.6	±3.1	±7.2	18.4	±3.3	±9.1	24.4	±0.7	±8.3
Annually	7.9	±2.0	±5.8	10	±2.1	±6.1	13	±1.9	±6.6

4.2.2 Angstrom turbidity analysis

It is found that for a variety of possible reasons, the fit of the measured relative transmittance to equation (3.36) can sometimes be insignificant, especially for lightly soiled glass coupons. The fit with a good R^2 value is plotted in Figure 4.10(a), and the direct transmittance of the clean glass is shown in Figure 4.10(c).

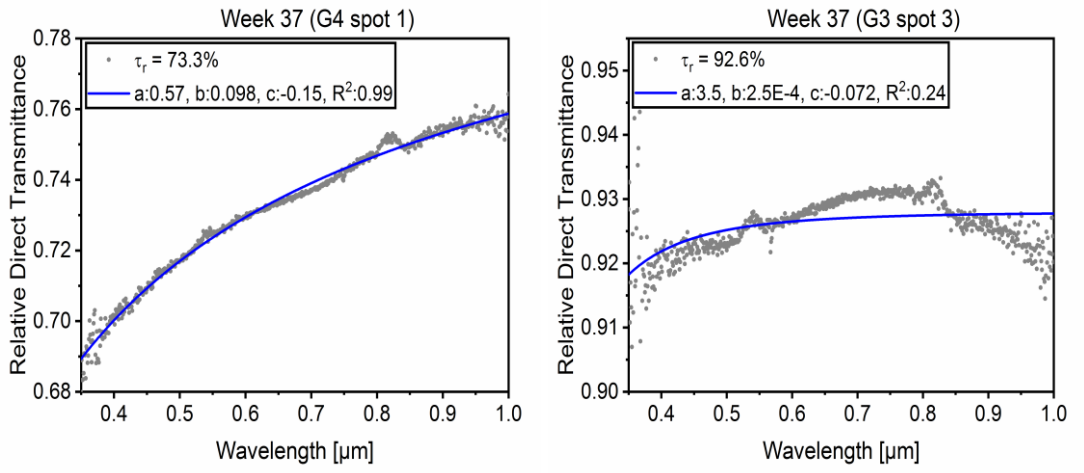

(a) (b)

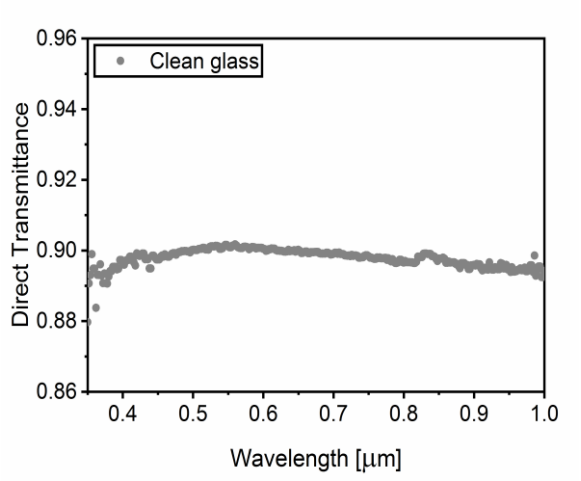

(c)

Figure 4.10 Examples of the direct relative transmittance data fit to the modified Ångström turbidity equation for glass coupons that exhibit (a) high R^2, (b) low R^2 values, and (c) direct transmittance of clean glass coupon with air as a reference. The data points are shown for the week and the spot on the coupon as indicated.

However, Figure 4.10(b) shows such a curve with a low R^2 value and an unexpected spectral shape. A plot of τ_r versus c is made in a similar way as reported in the previous study [180] to confirm the shape of the curve for multiple measurements. The selection criteria considered for the modified Ångström equation fit are as follows: if the R^2 for the fit is less than 0.70 and the spectral transmittance data has more than 5 points in the range 0.35 to 0.4 μm greater than 1/2 of the spectral transmittance value at 1 μm, then the result can be discarded as an outlier (for example, see Figure 4.10(b)). The average relative direct transmittance and the offset value, c, obtained from the modified Ångström turbidity equation for some weeks of the year and winter season is displayed in Figure 4.11. The plot shows a good R^2 value. These exercises indicate that, for the most part, the transmittance data are of good quality and sufficient for the analysis that is conducted with it.

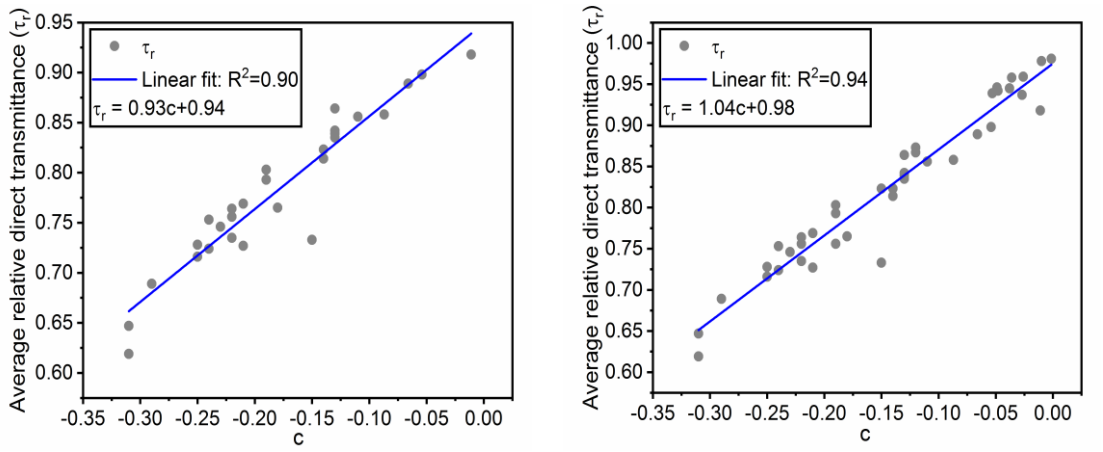

Figure 4.11 The average relative direct transmittance (τ_r) versus offset parameter, *c*, of the modified Ångström turbidity equation for (a) selected weeks of the whole year and (b) the winter season.

4.2.3 F-test and t-test analysis

The t-test (two-sample assuming unequal variance) is carried out to determine the statistically meaningful differences in net soiling on a seasonal basis. Following the methodology of F-test and t-test analysis in section 3.3. It is observed that there is no statistical difference in the net soiling when the glass coupons are either monthly or never cleaned, irrespective of whether it is analyzed on a seasonal basis or an annual basis. During the SW monsoon season, the statistical difference in net soiling could be seen when the glass coupon is cleaned weekly or left uncleaned. However, the difference is insignificant for other seasons. The net soiling during winter and post-monsoon seasons are statistically the same irrespective of different cleaning cycles. A week-long exposure during post-monsoon and winter can decrease the transmittance of glass coupons to values as low as those for a coupon that is never cleaned. Therefore, frequent cleaning (once a week) during post-monsoon and winter seasons is recommended to maintain high transmittance. However, cleaning once a month during pre-monsoon and SW monsoon season is found to be enough to maintain high transmittance because a week of exposure does not reduce the transmittance of glass coupons by much when compared to a month's exposure or when the coupon is never cleaned. For the site under study, the seasonal F- and t-test statistical analyses for combinations of cleaning cycles are shown in Table 4.3.

Table 4.3 The F-test and t-test (two sample results assuming unequal variance) statistical analysis for different combination of glass coupons. The results compare the weekly cleaned (G2), monthly cleaned (G3), and never cleaned (G4) glass coupons.

Season	**Combination of Glass Coupons**					
	G2–G3		**G2–G4**		**G3–G4**	
	F-test	**t-test**	**F-test**	**t-test**	**F-test**	**t-test**
Pre-monsoon	x	x	x	✓	x	x
SW monsoon	x	✓	x	✓	x	x
Post-monsoon	x	x	x	x	x	x
Winter	x	x	x	x	x	x
1 Year	x	x	x	✓	x	x
Non-monsoon	x	x	x	✓	x	x
High-soiling	x	x	x	✓	x	x
Low-soiling	x	✓	✓	✓	✓	x

- ✓: F/t-test null hypothesis is rejected (significant difference in the variance/means).
- x: F/t-test null hypothesis cannot be rejected (no significant difference in the variance/means).
- Non-monsoon season includes winter, pre-monsoon, and post-monsoon seasons.
- High-soiling season includes week 24 until week 46.
- Low-soiling season includes weeks 1–23 and weeks 47–52.
- The low-soiling and high-soiling seasons are classified based on the rainfall intensity received. The weeks with high rainfall are in the low-soiling season and weeks with low or no rainfall are in the high-soiling season.

The F- and t-test statistical analysis for all cleaning cycles showed that during winter and post-monsoon seasons have a significant difference in net soiling compared to the SW monsoon season. However, the difference is insignificant between winter and post-monsoon seasons; and the same is observed between post-monsoon and pre-monsoon seasons as well. Weekly cleaning and no cleaning during the pre-monsoon and SW monsoon seasons showed clear differences in the mean values, whereas monthly cleaning showed no significant difference in their mean values. The t-test analysis between different seasons for different cleaning cycles is presented in Figure 4.12.

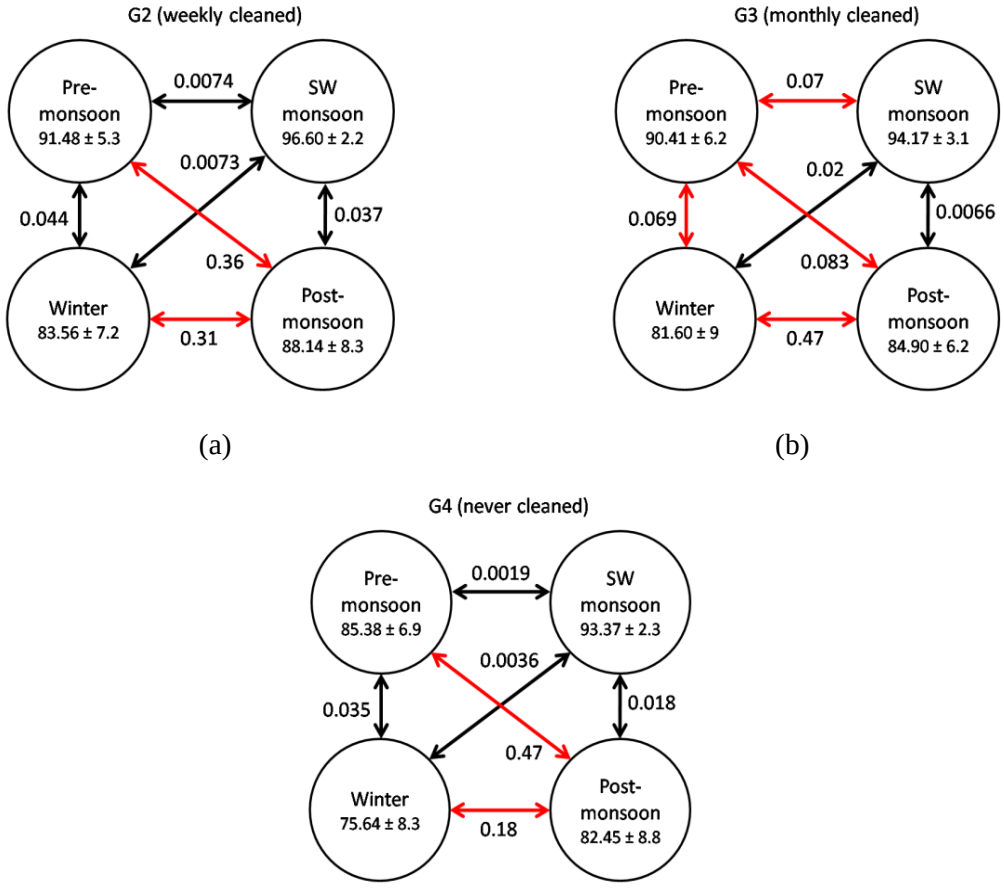

Figure 4.12 The t-test p-value of a combination of seasons for the weekly cleaned (G2), monthly cleaned (G3), and never cleaned (G4) glass coupons.

In Figure 4.12, the relation between two seasons connected with a red arrow does not have a statistically significant difference in their mean values (p-value > 0.05), whereas those connected with a black arrow have a statistically significant difference in their mean values (p-value < 0.05). The mean values for the transmittance are indicated along with their SD values. It could be seen that for a weekly cleaned glass coupon, G2 (Figure 4.12 a), there exist statistical significant difference in mean values between pre-monsoon and SW monsoon, pre-monsoon and winter, SW monsoon and winter, and between SW monsoon and post-monsoon. Therefore, SW monsoon is found to be statistically different from all other seasons. For the monthly cleaned, G3 (Figure 4.12 b), there exist statistical significance difference in the mean values between SW monsoon and winter and SW monsoon and post-monsoon. Whereas, there exist no statistically difference amongst the other

seasons. For the never cleaned glass coupon, G4 (Figure 4.12 c), the statistical significant difference could be observed amongst the seasons as similar to that of weekly cleaned glass coupon, G1. A statistical significant difference between the SW monsoon season and all other season is observed. Therefore, the seasons are divided into two categories: monsoon (SW monsoon) versus non-monsoon (includes post-monsoon, winter, and pre-monsoon) and low-soiling versus high-soiling seasons to analyze the difference between the cleaning cycles.

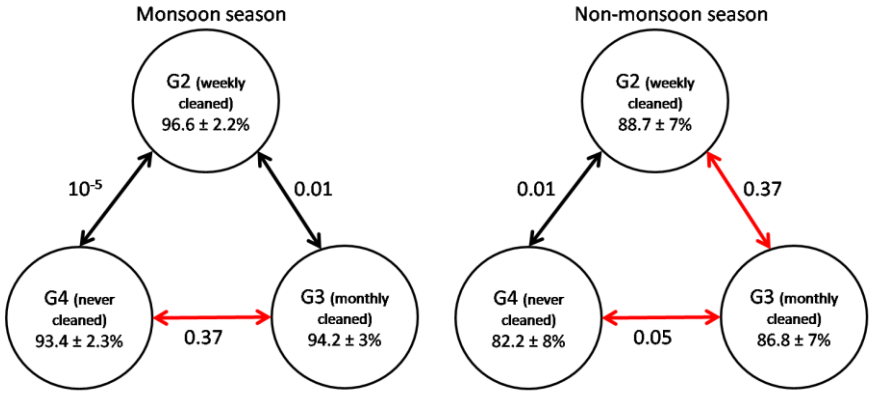

Figure 4.13 The t-test analysis between different cleaning cycles: weekly cleaned, monthly cleaned, and never cleaned glass coupons for the monsoon (left) and non-monsoon (right) seasons.

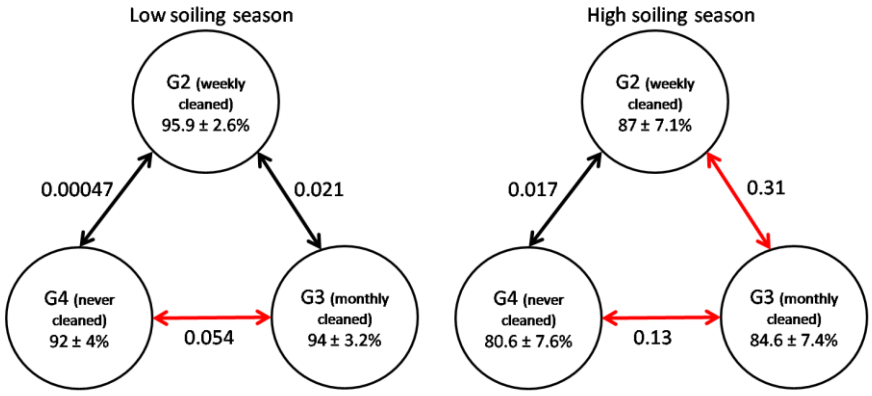

Figure 4.14 The t-test analysis between different cleaning cycles: weekly cleaned, monthly cleaned, and never cleaned glass coupons for the low-soiling (left) and high-soiling (right) seasons.

As shown in Figure 4.13, weekly cleaned and never cleaned glass coupons are statistically different during monsoon and non-monsoon seasons, whereas, monthly

cleaned and never-cleaned glass coupons are statistically similar. It is observed that weekly cleaned and monthly cleaned glass coupons are statistically different during monsoon season and statistically similar during non-monsoon season. Similar statistical results are observed during the low-soiling and high-soiling seasons, as summarized in Figure 4.14. Had this statistical approach not been employed, erroneous conclusions might have been made, and conclusions that are on more solid footing might have been overlooked. The results of Figures 4.13 and 4.14 are summarized in Table 4.3.

4.2.4 Cleaning cycles

The seasonal τ_{loss} of the glass coupons G2, G3, and G4 during various seasons over the year is shown in Figure 4.15. These average values are also presented in Table 4.2. The annual average loss due to soiling is 7.9%, 10%, and 12.9% for weekly (G2), monthly (G3), and never (G4) cleaning cycles, respectively. As discussed earlier, in section 4.2.3 from the statistical F-test and t-test analysis, recommendations are made regarding the cleaning cycle on a seasonal basis. Therefore, in a warm and wet monsoon, dry winter, and a high *RH* location like Tezpur, weekly cleaning can maintain a high weekly τ_r above 80% during post-monsoon and winter seasons, while

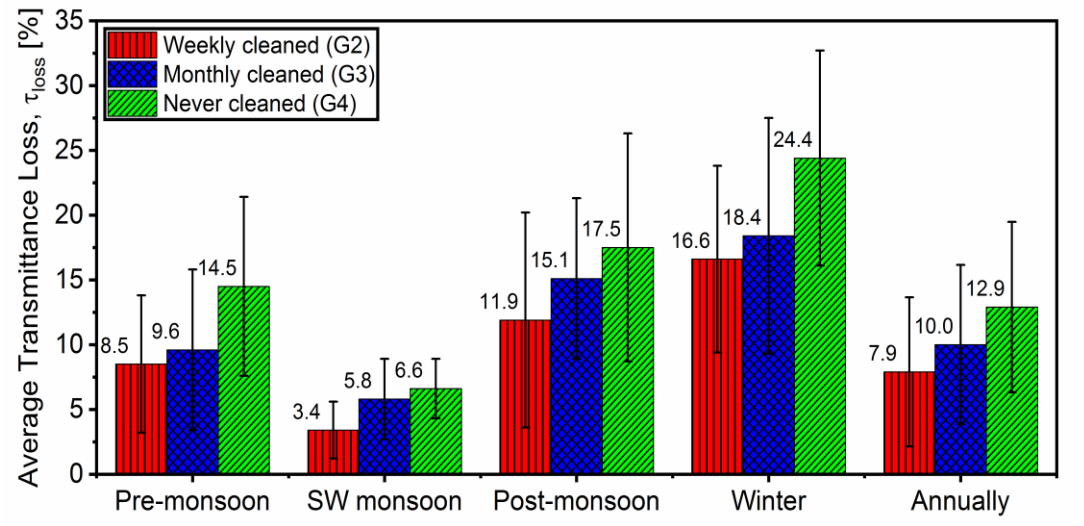

Figure 4.15 Seasonal average transmittance loss (τ_{loss}) and the respective standard deviation (in %) of weekly cleaned (G2), monthly cleaned (G3), and never cleaned (G4) glass coupons during the four seasons.

monthly cleaning can maintain the weekly τ_r above 90% during pre-monsoon and SW monsoon seasons. The cleaning cycle recommendation in this research work are made based on the transmittance measurement of the glass coupons (which acts a proxy to the PV glass cover) in different seasons due to soiling. The other parameters like cleaning process and expenditure involved in cleaning may be taken into consideration in the future studies.

4.2.5 Effect of environmental parameters on PV soiling

The environmental parameters are found to have significantly affected the soiling in the PV module based on location. In this work, the effect of individual and combination of environmental parameters (such as rainfall, rainfall frequency, relative humidity, wind speed, wind direction, air temperature, dew point temperature, and particulate matter) on PV soiling (τ_r value of the glass coupons exposed to natural soiling) is determined. The effect of the environmental parameters on the τ_r value of the glass coupons has been analyzed to understand the impact of these environmental parameters on PV soiling at the location under study. This part of the recommended methodology is outlined in the bottom half of the flowchart given in Figure 3.8. Hence, a correlation between the relative direct transmittance and the environmental parameters has been derived based on seasonality and annually.

4.2.5.1 Effect of rainfall on transmittance

The correlation between the τ_r and R_{max} for the G2, G3, and G4 glass coupons are shown in Figure 4.16(a)-(c). The R_{max} for each week is obtained as the maximum hourly rainfall intensity. Following the previous finding of a study conducted in Qatar by Javed et al. [69], a nonlinear function of the logistic type is modeled to fit the correlation between average weekly τ_r and R_{max}. However, the correlation did not achieve high R^2 values (0.42 for G2, 0.40 for G3, and 0.39 for G4). This might be due to the simultaneous effect of other environmental parameters on soiling. The winter season is 'dry' and hardly receives any rainfall, showing the lowest R_f compared to other seasons. As shown in Figure 4.16(d), it could be observed that the slope of the logistic fit in the case of G2 and G3 is not as steep as in G4. Also, the maximum limit of τ_r is highest for G2, followed by G3 and G4. The threshold rainfall (defined as 95% of the limit of the logistic function describing the correlation between τ_r and rainfall)

is calculated for all the glass coupons. There exists a minimum threshold, and it depends on the cleaning strategy. The threshold rainfall of G4 is 2.1 mm/hr, which suggests that the loose dirt is knocked off the glass surface with even less rainfall than the other coupons. Even with the hardest rainfall, we do not achieve a relative transmittance equal to weekly cleaning or even monthly cleaning. With its manual weekly cleaning, G2 has a high threshold rainfall of 3.4 mm/h, and G3 (manually monthly cleaned) has a value of 3.1 mm/h, as shown in Figure 4.16(d). The values of the parameters obtained from the logistic curve fit of Figure 4.16 are provided in Table 4.4.

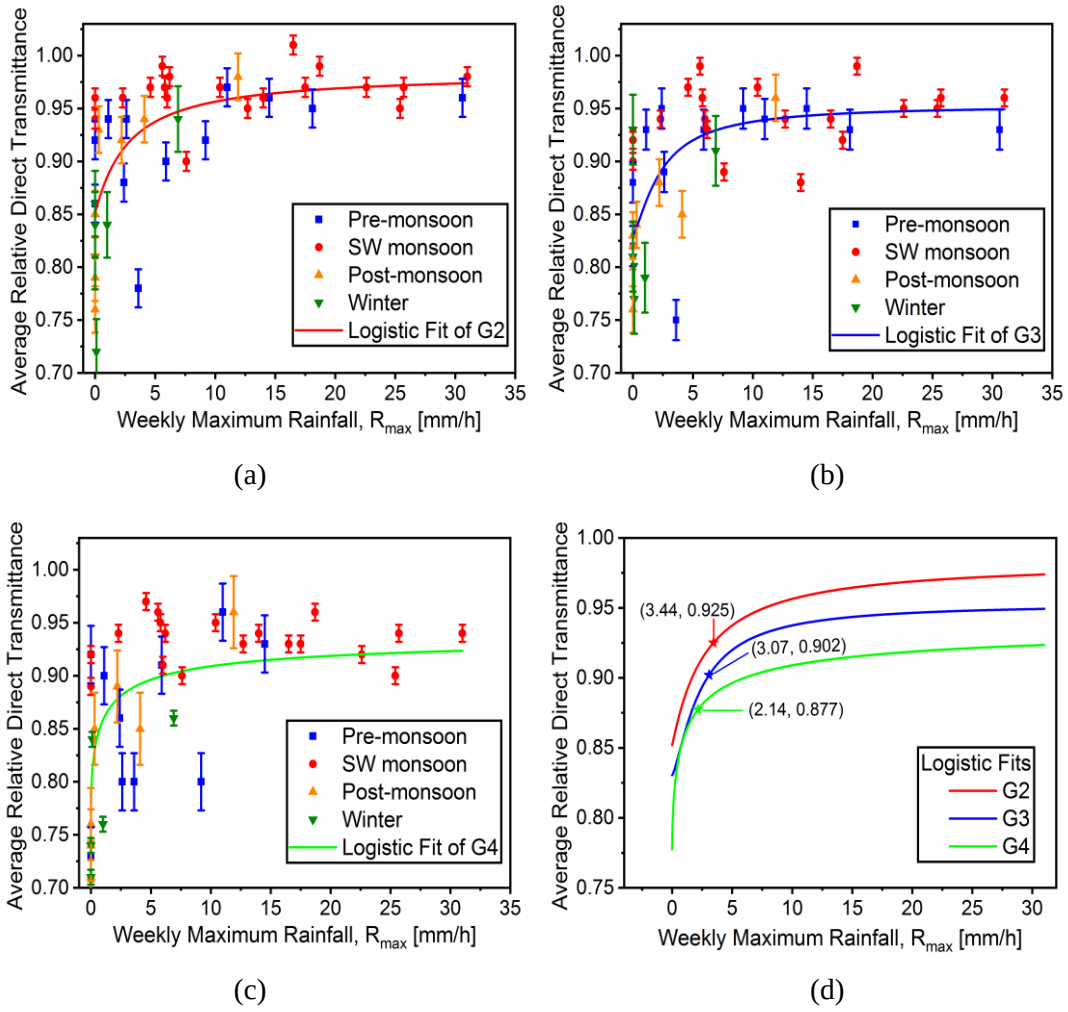

Figure 4.16 The average relative direct transmittance versus the weekly maximum rainfall (R_{max}) for the (a) G2 (R^2 = 0.42), (b) G3 (R^2 = 0.40), (c) G4 (R^2 = 0.39) and (d) the threshold rainfall required to clean the glass coupon under various cleaning schedule.

Table 4.4 The value of the indicated parameters and the R^2 value obtained from the logistic curve fitting [69] for the average relative direct transmittance of the glass coupons vs. the weekly maximum rainfall R_{max}, for different cleaning cycles: G2, G3 and G4.

Equation: τ_r =A2+(A1-A2)/(1+(R_{max}/x0)^q)							
Glass Coupon	**A1**	**A2**	**x0**	**q**	**Reduced Chi-square**	**R-squared**	**Adjusted R-squared**
G2	0.85	0.98	2.78	1.06	0.0027	0.46	0.42
G3	0.83	0.95	2.40	1.34	0.0030	0.45	0.41
G4	0.78	0.94	1.05	0.62	0.0044	0.43	0.39

4.2.5.2 Correlation between relative transmittance, PM10, and relative humidity

The location of this study has remarkably high *RH*, always > 70% throughout the year. This may lead to increased soiling. Previous studies [233, 245] reported that, for *RH* > 80%, the dust particle removal rate is low because of the water capillary bridges

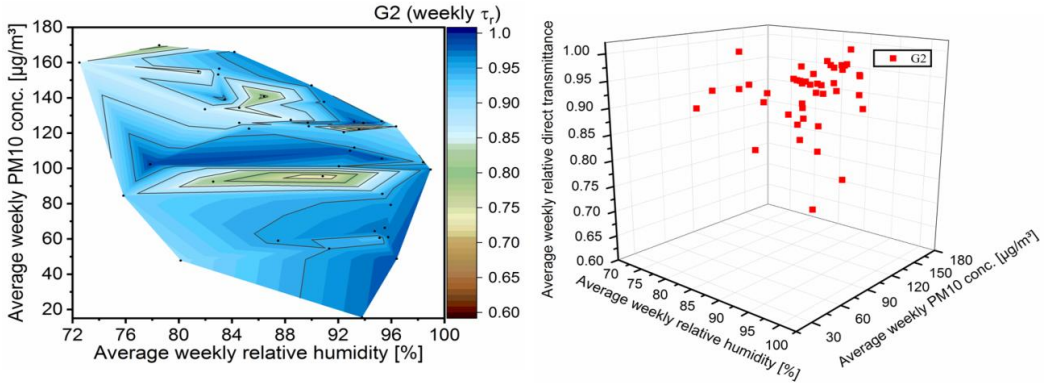

(a)

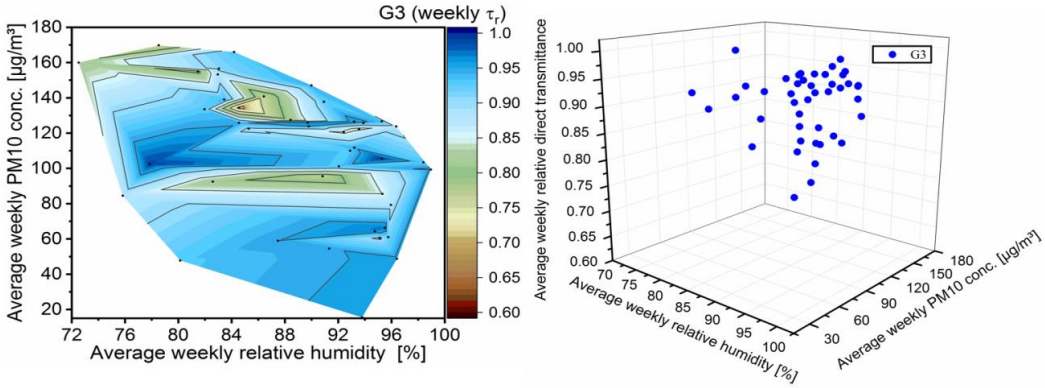

(b)

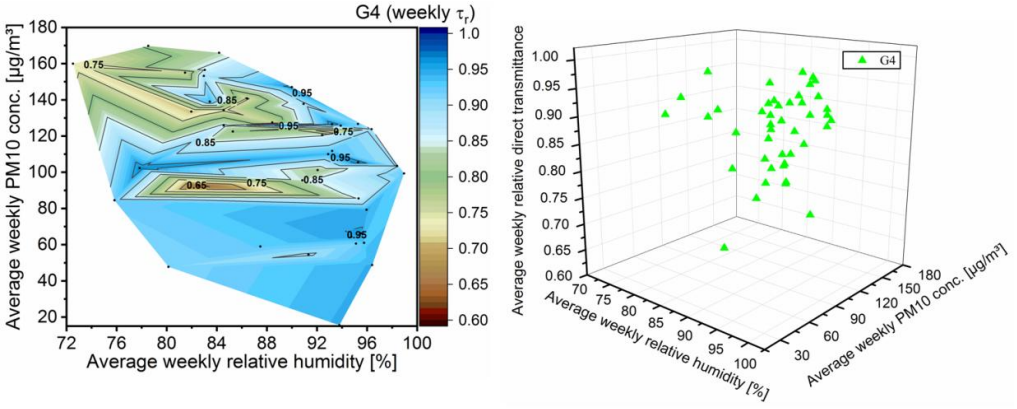

(c)

Figure 4.17 Correlation between the average relative direct transmittance (τ_r), the average weekly *PM10*, and *RH* for the glass coupon with different cleaning cycles: (a) G2, (b) G3, and (c) G4. The figure on the right shows the scatter plot for data on the left.

formed between the particles and the glass surface due to the presence of condensed water. Therefore, the impact of *RH* on soiling may be significant in the location under study. In addition to *RH*, another factor defining the severity of soling is the particle concentration (*PM10*) in the atmosphere. At the investigated site, *RH* ranged between 72% and 98%. Soiling is found not to be significant for *PM10* < 80 µg/m^3; however, with *PM10* in the range of 80-120 µg/m^3, maximum τ_{loss} is observed for all the glass coupons. For *PM10* above 120 µg/m^3, the severity of soiling increases when the glass coupons are kept uncleaned, as shown in Figure 4.17(a)-(c). However, no significant correlation between *RH*, *PM10*, and τ_r is obtained simultaneously using all the measurements recorded during a year. The plot on the right of Figure 4.17(a)-(c) is the scatter plot of data on the right of same figure. The scatter plot gives a clearer picture of distribution of plots on the left (contour plot). For instance, it may happen that the number of points or data representing severe or low soiling may be only one or two, which may not be conclusive interpretation.

4.2.5.3 Correlation between relative transmittance and air temperature

For T_{amb}, p<0.05 is found with R^2 adjusted values of 0.50, 0.47, and 0.60 for G2, G3, and G4, respectively. The parameters obtained from the linear fitting of τ_r and T_{amb} is provided in Table 4.5. It is observed that with an increase in T_{amb}, transmittance increases (the surface gets cleaner). Since the weekly average of T_{amb} lies in the range from 21°C (monsoon) to 6°C (winter), it might be the effect of the

thermophoresis force (explained in a later section) for this behavior. However, no significant correlation could be drawn between the transmittance and W_s.

Table 4.5 The value of the indicated parameters and the R^2 value obtained from the linear curve fitting for the average relative direct transmittance (τ_r) vs. average air temperature (T_{amb}) for the weekly cleaned (G2), monthly cleaned (G3), and never cleaned (G4) glass coupons for the whole year.

Equation: τ_r= Slope·T_{amb}+ Intercept						
Glass coupons	**Intercept**	**Slope**	**Residual sum of squares**	**Pearson's coefficient**	**R-squared**	**Adj. R-squared**
G2	0.76 ± 0.026	0.011 ± 0.0017	0.10	0.72	0.52	0.50
G3	0.73 ± 0.027	0.011 ± 0.0018	0.11	0.70	0.48	0.47
G4	0.65 ± 0.029	0.016 ± 0.0019	0.12	0.78	0.61	0.60

4.2.5.4 Correlation between relative transmittance, PM10, and dew point temperature

Another parameter influencing soiling that is related to *RH* is dew formation, which is a result of condensation. Dew forms on a surface with a temperature lower than the atmosphere, especially at night with a clear sky having suitable conditions for radiative cooling [55, 233]. Over the year, the experiment recorded the average weekly ΔT < 6°C, suggesting that the dew might occur frequently at the site. The average weekly ΔT is the difference between the average weekly ambient air temperature (T_{amb}) and average weekly dew point temperature (T_d). The impact of ΔT and *PM10* on τ_r for the glass coupon G2 is shown in Figure 4.18. The correlation is similar to the correlation obtained between the *RH*, *PM10*, and τ_r. It is observed empirically that condensation occurred on glass surfaces whilst the combined conditions such as high *RH* and $T_d \geq (T_{amb} - 2.5°C)$ are met, as in Figure 4.18(b). This is given by the number of hours in a week. It is observed that all the days of the week meet the condition at least for a few hours. For the correlation of τ_r with T_d, refer to Table 4.6. This is taken into consideration to explore the process of dew formation, which could increase soiling by various mechanisms such as particle adhesion, cementation, and particle caking [55].

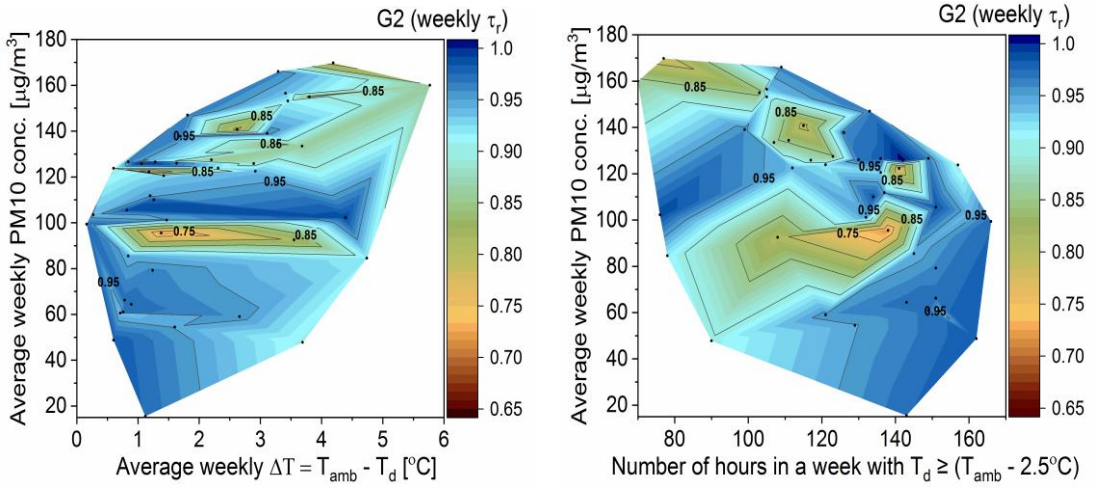

Figure 4.18 Relation between average weekly relative direct transmittance (τ_r), average weekly *PM10* concentration, and (a) average weekly ΔT, and (b) the number of hours in a week with the condition $T_d \geq (T_{amb} - 2.5°C)$ for the weekly cleaned glass coupon G2.

Table 4.6 The value of the indicated parameters and the R^2 value obtained from the linear curve fitting for the average relative direct transmittance (τ_r) vs. the average dew point temperature (T_d) for G2, G3, and G4 glass coupons for the whole year.

Equation: τ_r = Slope·T_d + Intercept

Glass coupons	Intercept	Slope	Residual sum of squares	Pearson's coefficient	R-squared	Adj. R-squared
G2	0.79 ± 0.019	0.010 ± 0.0015	0.09	0.74	0.54	0.53
G3	0.77 ± 0.021	0.010 ± 0.0016	0.11	0.71	0.50	0.49
G4	0.70 ± 0.020	0.014 ± 0.0015	0.10	0.82	0.67	0.66

The yearly analysis carried out using an SLR model showed $p < 0.05$ for the correlation between τ_r for different glass coupons and the individual environmental parameters. The details of the parameter value from the fits between the average relative direct transmittance of the weekly cleaned glass coupon (G2) and the average weekly value of various environmental parameters refer to Table 4.7.

Table 4.7 The correlation values obtained using single-variable linear regression (SLR) models between the average relative direct transmittance of the weekly cleaned glass coupon (G2) and the average weekly value of various environmental parameters: rainfall intensity (*Rain*), frequency of rainfall (R_f), relative humidity (*RH*), particulate matter (*PM10*), ambient air temperature (T_{amb}) and dew point temperature (T_d). The analysis is performed using the data for a full year.

1-year analysis using SLR model

Environmental parameters	R-squared	Adj. R-squared	Standard Error	Correlation
Rain	0.26	0.24	0.060	$\tau_r = 0.0068\ Rain + 0.89$
R_f	0.27	0.26	0.059	$\tau_r = 0.016\ R_f + 0.88$
R_{max}	0.31	0.29	0.058	$\tau_r = 0.0043\ R_{max} + 0.89$
RH	0.15	0.13	0.064	$\tau_r = 0.0041\ RH + 0.56$
PM10	0.10	0.07	0.066	$\tau_r = -0.00058\ PM10 + 0.98$
T_{amb}	0.52	0.51	0.048	$\tau_r = 0.011 T_{amb} + 0.76$
T_d	0.56	0.55	0.046	$\tau_r = 0.011 T_d + 0.79$

However, the R^2 value is very low, signifying poor correlation. Therefore, an MLR method is utilized to analyze the combined impact of different environmental parameters on a seasonal and yearly basis on the average relative transmittance (τ_r) of the weekly cleaned (G2) glass coupon. This will be presented in the next section. The glass coupons G2 and G3 are not analyzed in the similar process because of the insignificant difference in the mean of the τ_r of different cleaning cycles on seasonal basis except for the SW monsoon season as evident from the t-test analysis.

4.2.6 Seasonal Correlation between different environmental parameters

In accordance with previous studies, the combined effect of *PM10* and R_f [190], of *Rain* and W_s [177], and of W_s and *RH* [167] are found to significantly affect soiling even at the investigated location. Based on the relation obtained between the input environmental parameters and the τ_r for different seasons of the year, the predicted and measured datasets are plotted to obtain a linear relation using the linear regression method as shown in Figures 4.19-4.21.

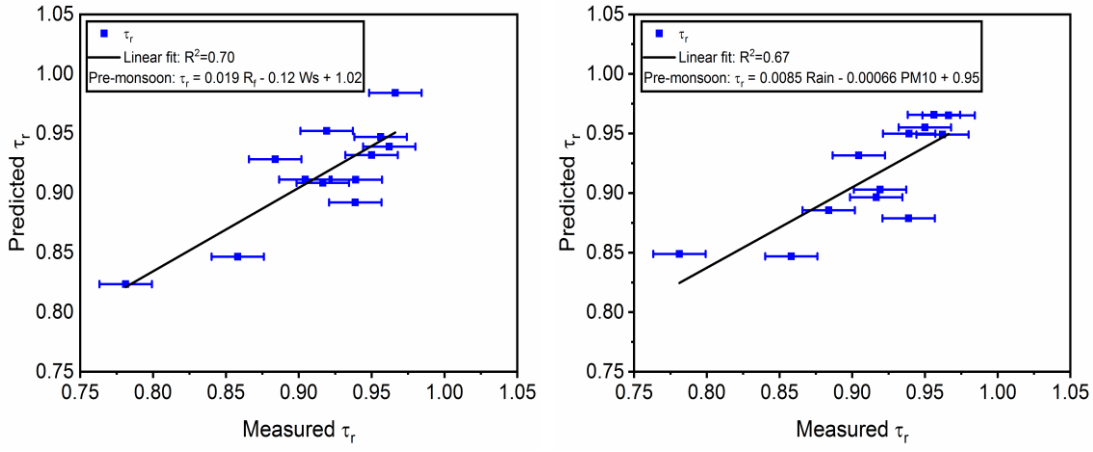

(a) (b)

Figure 4.19 Regression plots of predicted transmittance and measured transmittance of weekly cleaned glass (G2) using an MLR model during the pre-monsoon season for various environmental parameters (a) R_f and W_s, and (b) *Rain* and *PM10*. The uncertainty associated with the average relative direct transmittance of the weekly cleaned glass coupon during pre-monsoon is ±0.018.

During the pre-monsoon season (Figure 4.19), two combinations are found to be significant: a) R_f and W_s (R_f showed a positive correlation and W_s showed a negative correlation with τ_r), and b) *Rain* and *PM10* (*Rain* showed a positive correlation and *PM10* showed a negative correlation). In the first case, an increase in R_f cleans, whereas an increase in W_s leads to the soiling of the glass surface. This may be rationalized by considering that frequent rainfall cleans the surface, and W_s in the range $\leq$ 4 m/s tend to deposit dust onto the surface [34, 167, 192]. In the second case, increases in *Rain* and reductions in *PM10* also increase τ_r (reduces soling) during the pre-monsoon season. Comparatively speaking, during this season, *PM10* concentration fluctuate the most, with the maximum and minimum values of 169.5 µg/m^3 and 50.5 µg/m^3, respectively.

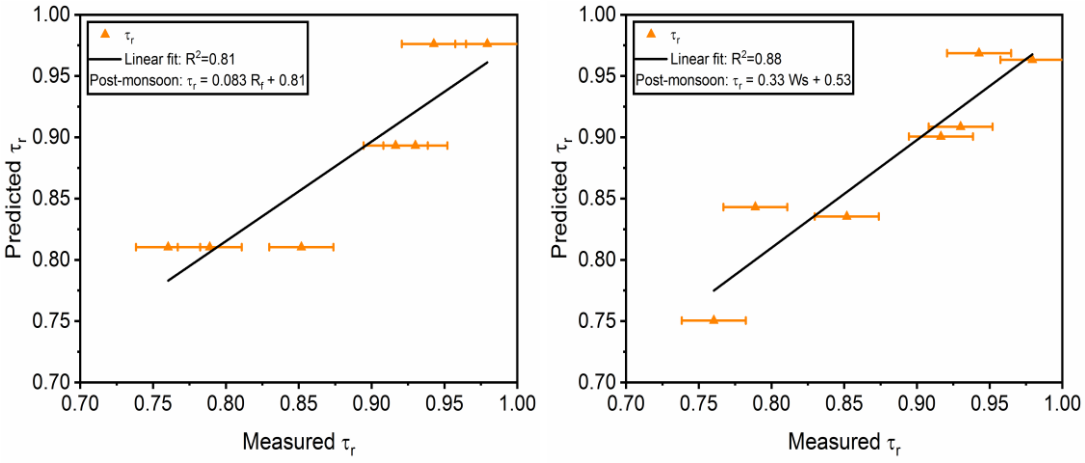

(a) (b)

Figure 4.20 Regression plot of predicted transmittance and measured transmittance of weekly cleaned glass (G2) using a MLR model during post-monsoon season for the environmental parameters: (a) R_f, and (b) W_s. The uncertainty association with the average relative direct transmittance of the weekly cleaned glass coupon during post-monsoon is ±0.022.

The analysis during post-monsoon season (Figure 4.20) showed that W_s and R_f have a positive correlation with τ_r but these two parameters affect the transmittance of G2 individually. They do not have interdependency on one another. High values of W_s results in the cleaning of the glass surface for low W_s in the range 0-2 m/s, as this range may not be sufficient to blow the surrounding soiling particles onto the glass surface [191].

During the winter season (Figure 4.21), the following is found: (a) *Rain* and W_s and (b) R_{max} and W_s showed a significant correlation. All the environmental parameters in both of the relationships that are determined showed a positive correlation. Increases in both *Rain* and W_s simultaneously increases τ_r during the winter season. W_s can have two effects on soiling, as reported by Sayyah et al. [177]. During post-monsoon and winter seasons, it showed a positive correlation, but a negative correlation is observed during pre-monsoon. Moreover, no significant relation between the transmittance and any of the environmental parameters is obtained during the SW monsoon season. Comparably higher *Rain* and R_f during that season lowers the chance of soiling and minimizes the impact of other environmental parameters.

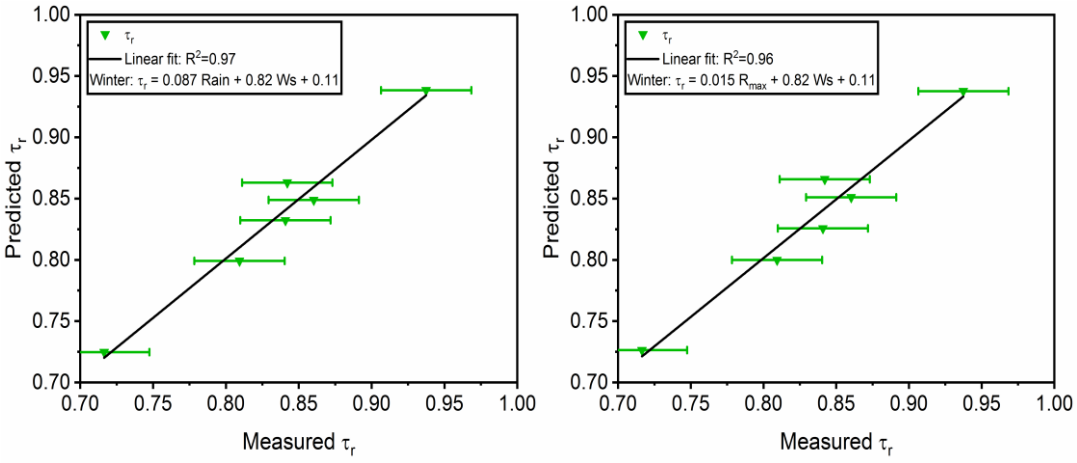

(a) (b)

Figure 4.21 Regression plot of predicted transmittance and measured transmittance of weekly cleaned glass (G2) using an MLR model during the winter season for various environmental parameters: (a) *Rain* and W_s, and (b) R_{max} and W_s. The uncertainty associated with the average relative direct transmittance of the weekly cleaned glass coupon during winter is ±0.031.

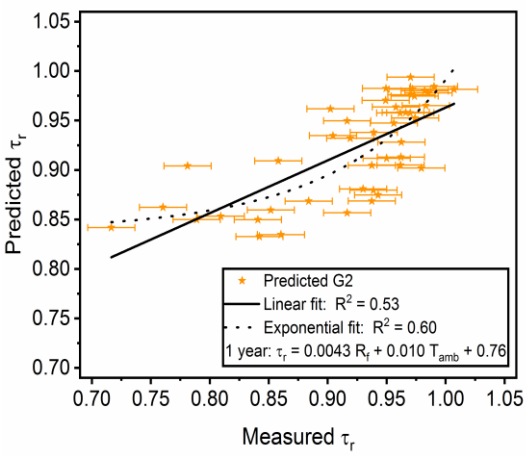

Figure 4.22 Regression plot of predicted transmittance and measured transmittance of weekly cleaned glass (G2) using an MLR model for a year. The uncertainty associated with the average relative direct transmittance of the weekly cleaned glass coupon is ±0.02. The solid line represents the linear fit, and the dashed line represents an exponential fit with an offset to guide the eye (For the values of parameters of the linear and exponential fits, refer to Tables 4.8 and 4.9, respectively.).

An analysis over the whole year (Figure 4.22) showed a positive correlation between τ_r and R_f and T_{amb} having a low R^2 value of 0.53. The value of the parameters obtained from linear and exponential fitting of Figure 4.22 is depicted in Tables 4.8 and 4.9, respectively. However, the correlation is found to be not significant.

Table 4.8 Values for the linear fit parameters for the annual analysis using MLR. This is used for the regression plot of predicted and measured transmittance for the weekly cleaned glass (G2) using an MLR model for the whole year.

Linear Fit: τ_r (Predicted) = Slope·τ_r (Measured) + Intercept					
Intercept	**Slope**	**Residual sum of squares**	**Pearson's coefficient**	**R-squared**	**Adj. R-squared**
0.42 ± 0.071	0.53 ± 0.077	0.05	0.73	0.53	0.52

Table 4.9 Values for the exponential fit parameters for the annual analysis using MLR. This is used for the regression plot of predicted and measured transmittance for the weekly cleaned glass (G2) using an MLR model for the whole year.

Exponential fit: τ_r (Predicted) = A· exp(B· τ_r (Measured)) + Offset					
A	**B**	**Offset**	**Reduced Chi-square**	**R-squared**	**Adj. R-squared**
7.5E-6 ± 3.3E-5	9.91 ± 4.17	0.84 ± 0.028	0.0010	0.60	0.58

With the high seasonality of the site, even the significance of correlations between soiling (quantified by the average transmittance) and environmental parameters changes with the season. Some parameters which show significance during one season may not have any significance in a different season. Moreover, these correlations are for the considered year of analysis; they may change when more data from two or more years are considered. The significant correlation between the τ_r and the environmental parameters for various seasons and annually is presented in Table 4.10.

Table 4.10 The seasonal analysis result of the MLR model in correlating the average relative direct transmittance of the weekly cleaned glass (G2) and the environmental parameters with p-value < 0.05.

Seasons	Input environmental parameters	R^2	Standard Error	Relation
Pre-monsoon	R_f and W_s	0.70	0.03	$\tau_r = 0.019\ R_f - 0.12\ W_s + 1.02$
	Rain and *PM10*	0.67	0.03	$\tau_r = 0.0085\ Rain - 0.00066\ PM10 + 0.95$
Post-monsoon	R_f	0.81	0.04	$\tau_r = 0.083\ R_f + 0.81$
	W_s	0.88	0.03	$\tau_r = 0.33\ W_s + 0.53$
Winter	*Rain* and W_s	0.97	0.02	$\tau_r = 0.087\ Rain + 0.82\ W_s + 0.11$
	R_{max} and W_s	0.97	0.02	$\tau_r = 0.015\ R_{max} + 0.82\ W_s + 0.11$
1-year	R_f and T_{amb}	0.53	0.05	$\tau_r = 0.0043\ R_f + 0.010\ T_{amb} + 0.76$

4.2.7 Electrical characterization of the PV module exposed to natural soiling

This part of the work follows the methodology provided in section 3.2.5. The glass coupon placed at 0° and 26° showed a similar trend of drop in relative transmittance value. The relative transmittance value for glass coupons placed at horizontal and tilted positions is shown in Figure 4.23. The relative transmittance value remained in the range of 1.0-9.0 throughout the year.

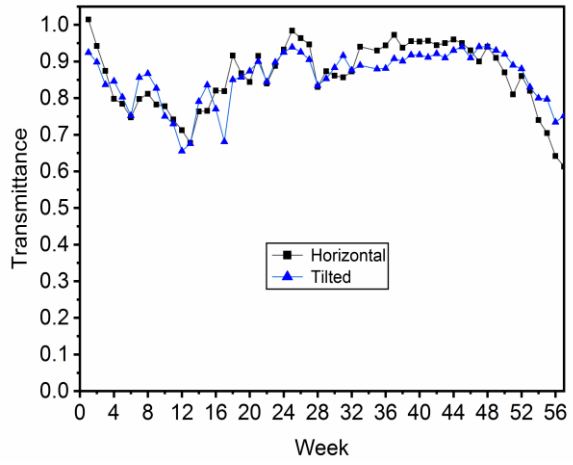

Figure 4.23 Relative transmittance of the glass coupon placed at horizontal (0°) and tilted (26°) angles under the never cleaned condition.

On the contrary, the relative transmittance value drops up to 0.65 (observed during the winter) for the glass coupons at the horizontal and tilted positions. At these positions, the relative transmittance value is found to be a maximum of 0.98 only, even with the prevailing self-cleaning situation such as high intensity rainfall during the SW monsoon season.

The relative transmittance and normalized efficiency, $\eta_{normalized}$ (equation 3.40) of the PV modules at horizontal and tilted angles, are shown in Figure 4.24. The trend between the relative transmittance and $\eta_{normalized}$ is quite similar, with a larger drop in transmittance value compared to the $\eta_{normalized}$. This may be due to greater deviation in light transmittance in glass coupons compared to PV modules because of higher ratio of non-uniform distribution of soiling and area under soiling in glass coupons compared to the PV module. Moreover, the seasonality may be the other attribute to these deviations, as greater deviation between the transmittance and $\eta_{normalized}$ is observed during the non-monsoon seasons.

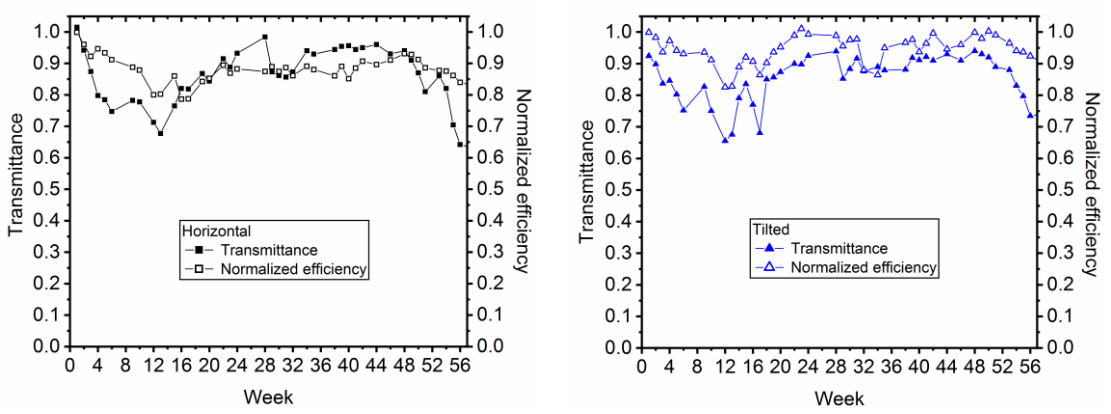

(a) (b)

Figure 4.24 Relative transmittance and normalized efficiency of the PV modules placed at (a) horizontal (0°) and (b) tilted (26°) angles.

The electrical performance of a PV module decreases with longer exposure of a PV module outdoors without any manual cleaning, as shown in Figure 4.25. It is observed that the percentage change in the $\eta_{normalized}$ between the clean module and the module placed at horizontal position after being exposed to the outdoor environment without any manual cleaning in week 5 is 4.3%, week 51 is 8.6%, and week 57 is

16.13% having the global horizontal irradiance 673.6 W/m^2. Thus, it is necessary to clean the PV module surface periodically based on the seasonal variation.

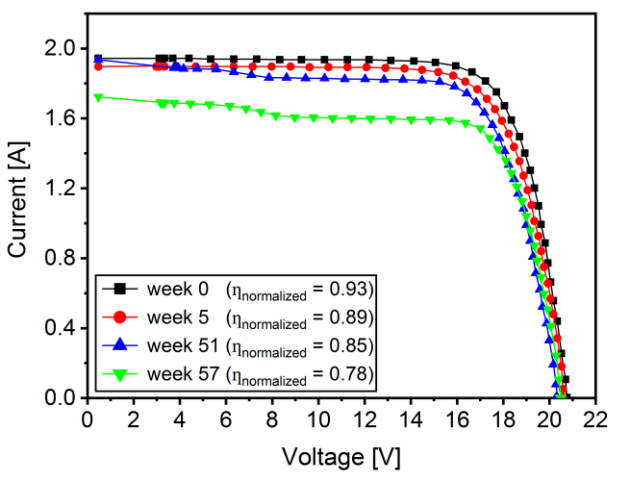

Figure 4.25 *I-V* curve of the soiled PV module (at horizontal position) for various weeks.

To determine the potential impact of soiling on the energy production of the PV module, the loss in energy generation of PV modules is calculated using equation (3.41) on a seasonal and annual basis under standard test conditions (STC). The results are shown in Figure 4.26 (The electrical specifications of the considered PV panel are tabulated in Table 3.4).

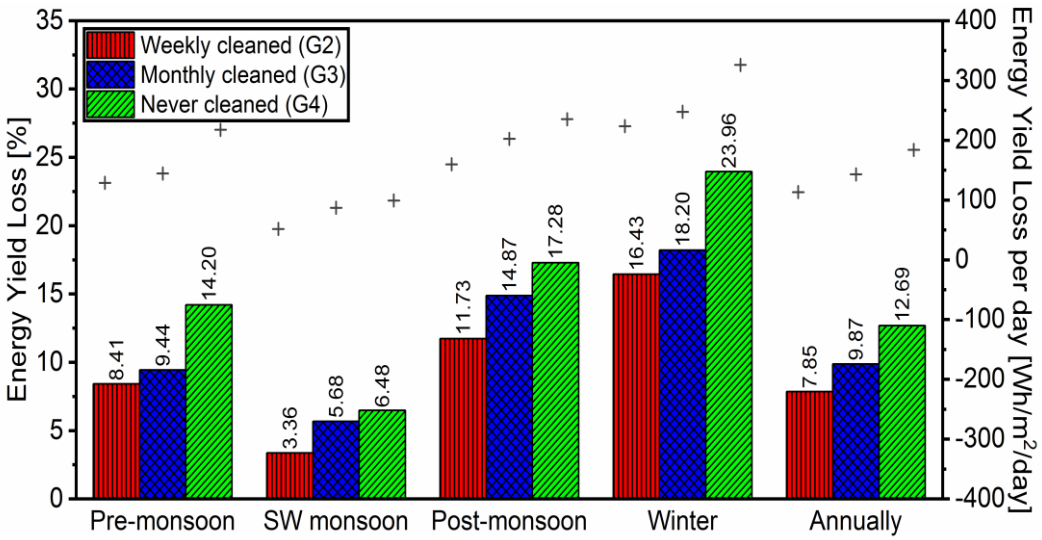

Figure 4.26. Energy yield loss percentage due to soiling for different cleaning cycles during the four seasons and annually at STC. The "+" symbol denotes the (predicted) energy yield loss in Wh/m^2/day for the right side y-axis.

It is found that the annual average E_{loss} due to soiling is 113.25 Wh/m^2/day (7.85%), 142.92 Wh/m^2/day (9.87%) and 183.98 Wh/m^2/day (12.69%) for weekly (G2), monthly (G3) and never (G4) cleaning cycles, respectively. On a seasonal basis, the E_{loss} observed from high to low is in the order of winter > post-monsoon > pre-monsoon > SW monsoon. In addition, the variation in the sunshine hour (H_s) within each season leads to the variation in the overall E_{loss} for a particular season. It could be observed that the τ_{loss} and E_{loss} are almost identical, with a slight difference during high soiling conditions. As these energy losses are calculated for the ideal conditions (Standard AM1.5D, a complete description should include the actual spectral irradiance distribution for the season. This is because in actual outdoor conditions, the spectral distribution, $G_D(\lambda,t)$ in equation (3.46), of the solar irradiance levels will vary, and so too will the E_{loss}.

4.3 Validation of the developed model using experimental results

In this section, the developed spectral, thermal, and electrical along with their integrated models are validated using the experimental data.

4.3.1 Validation of the spectral model

The simulated global spectral irradiance (G_{sim}) is experimentally (G_{exp} measured using spectrometer and pyranometer) validated diurnally with 5 minutes interval for the local time period 7:30 to 16:00 considering the seasonal variability. For instance, this

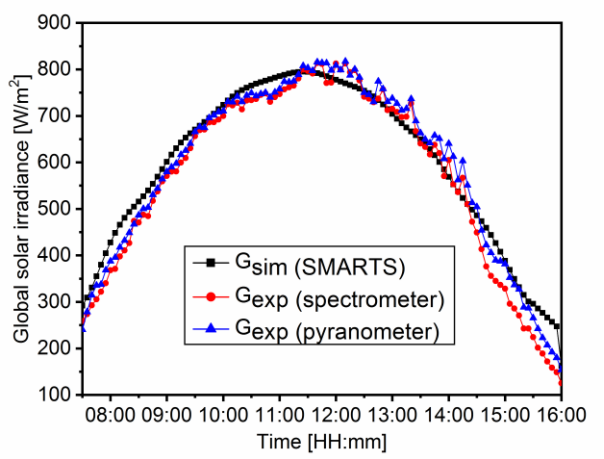

Figure 4.27 Comparison of the simulated spectral irradiance generated using SMARTS and the measured spectral irradiance using spectrometer and pyranometer.

validation considering the representative day of the pre-monsoon season is shown in Figure 4.27. Since crystalline PV modules are considered for the study, the model is validated for the wavelength range 300-1100 nm. A linear fitting between the predicted and measured global tilted irradiance is plotted to determine the closeness of the predicted value with the measured value for representative days of various seasons, as shown in Figure 4.28.

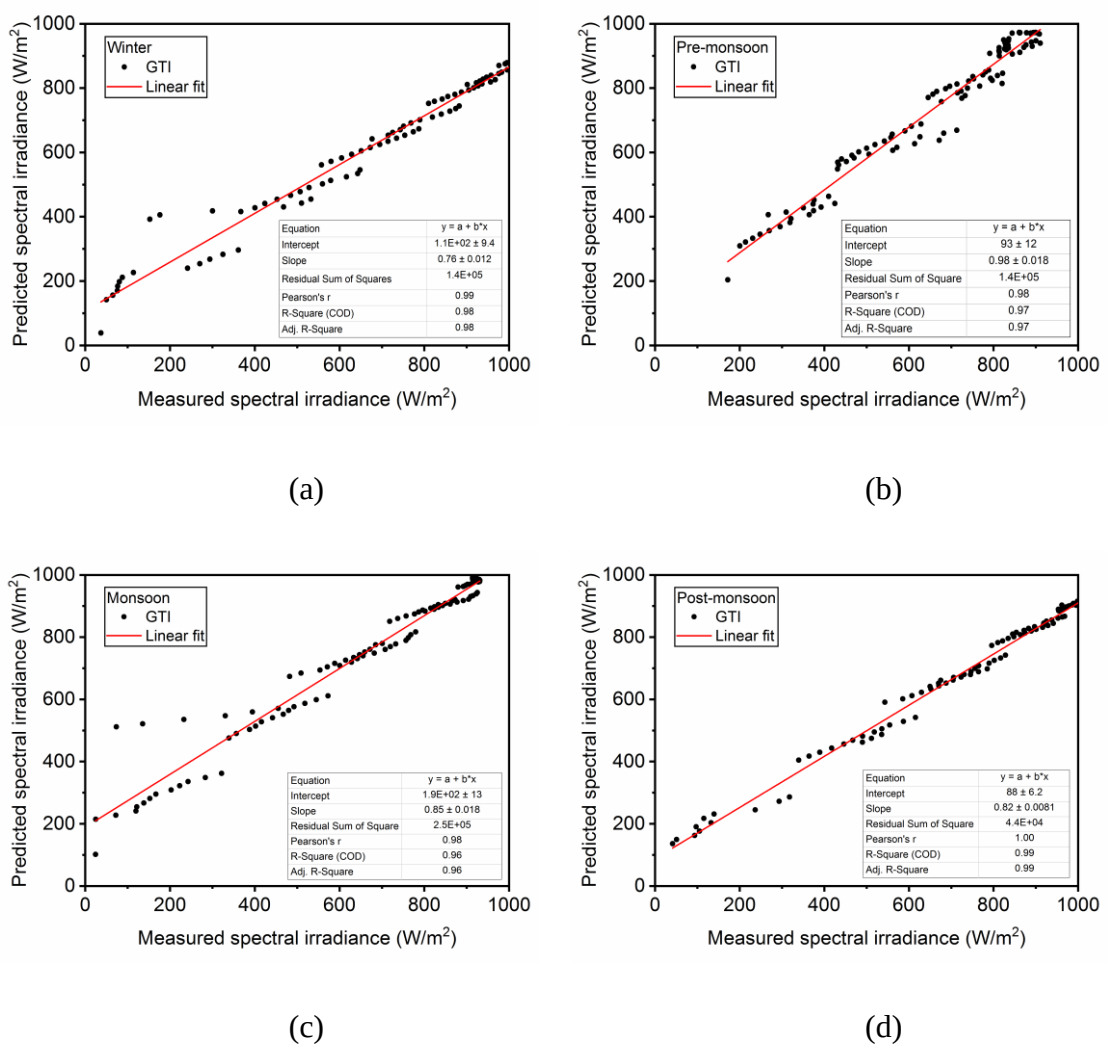

(a) (b)

(c) (d)

Figure 4.28 The linear fit between the predicted and measured global tilted irradiance (GTI) for (a) winter, (b) pre-monsoon, (c) SW monsoon, and (d) post-monsoon seasons. The R^2 of the predicted and measured spectral irradiance values for various seasons are presented in Table 4.11.

The average values of the simulated and measured global irradiance; and the coefficient of determination (R^2) from the linear fit for representative days of various seasons are shown in Table 4.11. The higher R^2 values (more that 0.95) has signified

the closeness of the simulated and experimental global irradiance over the day during different seasons.

Table 4.11 Average value of the simulated and measured global tilted irradiance and coefficient of determination (R^2) value.

Seasons	**Average G_{sim} (W/m^2)**	**Average G_{exp} (W/m^2)**	**R^2**
Winter	658.80	727.70	0.98
Pre-monsoon	733.20	656.00	0.97
SW monsoon	739.50	647.70	0.96
Post-monsoon	681.10	721.70	0.99

4.3.2 Validation of the thermal model

The validation of the thermal model is carried out as per the methodology discussed in section 3.4. Figure 4.29(a)-(d) shows the variation in measured T_c of the PV module with variations in the global tilted irradiance (GTI), $W_{s,}$ and T_{amb} for various days representing the seasons of a year. It is observed that during the representative winter day, the GTI is maximum with the average value of 727.7 W/m^2. The average GTI value during pre-monsoon, SW monsoon, and post-monsoon days is 656.0 W/m^2, 647.7 $W/m^{2,}$ and 721.7 W/m^2, respectively. The average daily ambient temperature during the winter, pre-monsoon, SW monsoon, and post-monsoon is 24.7°C, 32.4°C, 28.8°C and 29.8°C, respectively and the wind blows with an average speed of 0.36 m/s, 0.33 m/s, 0.22 m/s, and 0.23 m/s, respectively. The effect of wind speed on cell temperature could be visibly seen during the SW monsoon day. During the noon hours of the day, with almost stable GTI and T_{amb}, the cell temperature is observed to fluctuate; may be because of the fluctuation in W_s. During this period, a sudden change in W_s from 0 m/s to 1.3 m/s (within a time span of 15 minutes) might have lead to change in cell temperature of the module by 3.3%. This is due to the fact that the wind blowing onto the surfaces of the PV module can contribute to the change in cell temperature. Increased wind speed tends to cool the surfaces of the module, thereby reducing the cell temperature.

Similarly, such fluctuations could be seen during other seasons. For example, during the winter and post-monsoon days, the GTI has a smooth trend. However, the result showed some peaks and deeps in the PV cell temperature. The cause of these variations is at hours when the T_{amb} and W_s fluctuated abruptly. During the winter day,

Table 4.12 Average value of W_s, T_{amb}, and T_c (for m-Si and p-Si PV modules) for during various season.

Season	**Average**			
	W_s **(m/s)**	T_{amb} **(°C)**	$T_{c\_m\_exp}$ **(°C)**	$T_{c\_p\_exp}$ **(°C)**
Winter	0.36	24.70	50.40	51.30
Pre-monsoon	0.33	32.40	56.20	54.40
SW monsoon	0.22	28.80	63.50	58.30
Post-monsoon	0.23	29.80	55.00	51.50

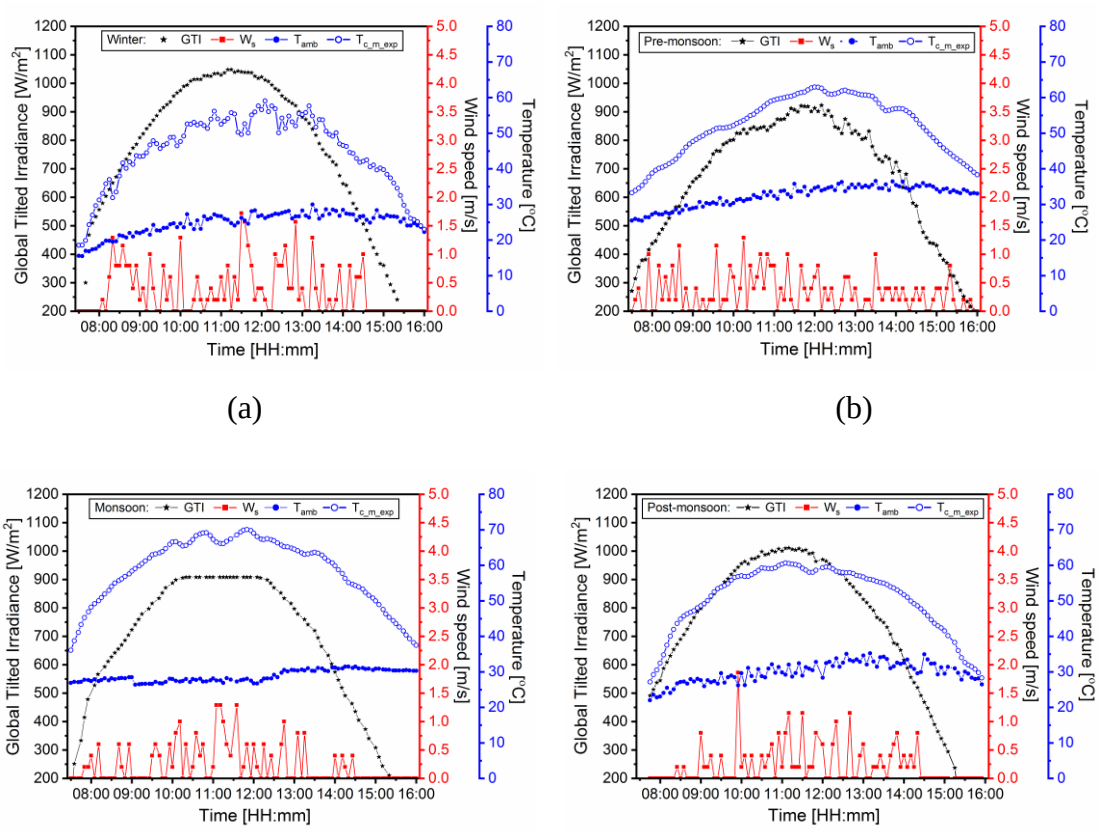

Figure 4.29 The variation in measured cell temperature ($T_{c\_m\_exp}$) of PV module with global tilted irradiance (GTI), wind speed (W_s), and ambient temperature (T_{amb}) during (a) winter, (b) pre-monsoon, (c) SW monsoon, and (d) post-monsoon.

a maximum of 13.2% change in T_c is obtained under instantaneous W_s reaches up to 1.3 m/s. The post-monsoon day showed a change of 4.3% in cell temperature under instantaneous W_s of 1.2 m/s. Moreover, during the pre-monsoon day, there is fluctuation in GTI, $W_{s,}$ and $T_{amb,}$ and the variations in T_c could be due to all the mentioned parameters. The average measured T_c for m-Si and p-Si and the average value of the environmental parameters W_s and T_{amb} for various seasons is tabulated in Table 4.12. The fluctuation in the solar spectrum, radiation, ambient air temperature, and wind speed throughout the day affects the variation in the cell temperature of the PV modules. It is observed that the variations in the meteorological conditions lead to an increase in the difference between the model and experimental data, also as mentioned in the previous work [246].

For the environmental parameters including wind speed and ambient temperature along with global tilted irradiance in Figure 4.29, the back temperature (T_b) of the PV module, which is directly measurable, is used to validate the thermal model. Considering T_b for validation of the thermal model avoids uncertainty. The T_b of the m-Si and p-Si PV modules is validated with the experimentally measured T_b for various seasons, as shown in Figure 4.30(a)-(d). The maximum rise in T_b is observed during the SW monsoon season, followed by pre-monsoon, post-monsoon, and least during winter for both m-Si and p-Si. It is found that the range of T_b changes with change in season. The range of T_b during winter is 36.31°C to 56.87°C for m-Si and 40.52°C to 58.61°C for p-Si, during pre-monsoon is 40.84°C to 62.56°C for m-Si and 39.66°C to 60.23°C for p-Si, during monsoon is 49.90°C to 68.7°C for m-Si and 44.8°C to 63.8°C for p-Si, and during post-monsoon is 41.31°C to 59.44°C for m-Si and 38.08°C to 57.57°C for p-Si. The plot also shows that, the simulated T_b have similar trend as the experimental T_b considering the varying environmental parameters. The MAE, MRE, RMSE, and R^2 values obtained from validation of T_b for both p-Si and m-Si are shown in Table 4.13.

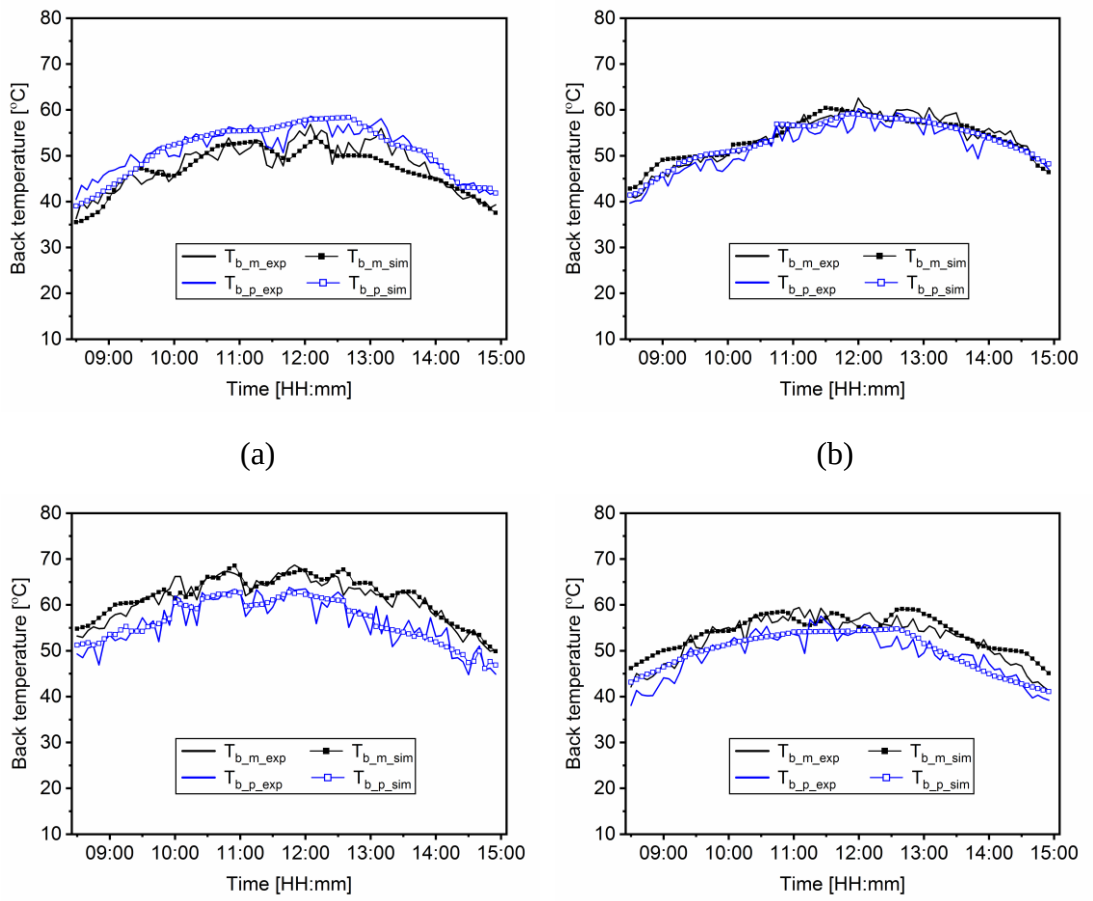

Figure 4.30 Validation of the simulated back temperature of PV modules with the experimental back surface temperature for various seasons: (a) winter, (b) pre-monsoon, (c) SW monsoon, and (d) post-monsoon (subscript '*b*' for back, '*m*' for m-Si, '*p*' for p-Si, '*sim*' for simulation and '*exp*' for experimental).

Table 4.13 Statistical errors of the developed thermal model in terms of T_b value for various seasons.

Season	**p-Si**				**m-Si**			
	MAE (°C)	**MRE**	**RMSE (°C)**	**R^2**	**MAE (°C)**	**MRE**	**RMSE (°C)**	**R^2**
Winter	1.55	0.04	2.05	0.88	1.95	0.04	2.46	0.80
Pre-monsoon	1.51	0.05	1.93	0.90	1.44	0.03	1.68	0.91
SW monsoon	1.69	0.03	2.15	0.84	1.28	0.02	1.67	0.90
Post-monsoon	1.83	0.04	2.29	0.81	2.16	0.04	2.59	0.82

Similarly, cell temperature (T_c) of the m-Si and p-Si PV modules is validated with the experimentally determined T_c (calculated using equation (3.62)) for different seasons, as shown in Figure 4.31(a)-(d). Here, T_c is a function of T_b and global

irradiance. The maximum rise in T_c is observed during the SW monsoon season, followed by pre-monsoon, post-monsoon, and least during winter for both m-Si and p-Si. It is observed that the simulated T_c has a similar trend as the experimental T_c. The simulate T_c is found to change with the varying GTI, W_s, and T_{amb}. The statistical errors (MAE, MRE, and RMSE) in simulated T_c are provided in Table 4.14. Therefore, from these error calculations and R^2 value, it is observed that the developed thermal model can be used to generate T_c under varying environmental parameters with good closeness to the experimental T_c. The RMSE ranges from 1.93°C to 2.29°C for m-Si and 1.67°C to 2.59°C for p-Si; with R^2 value above 0.80.

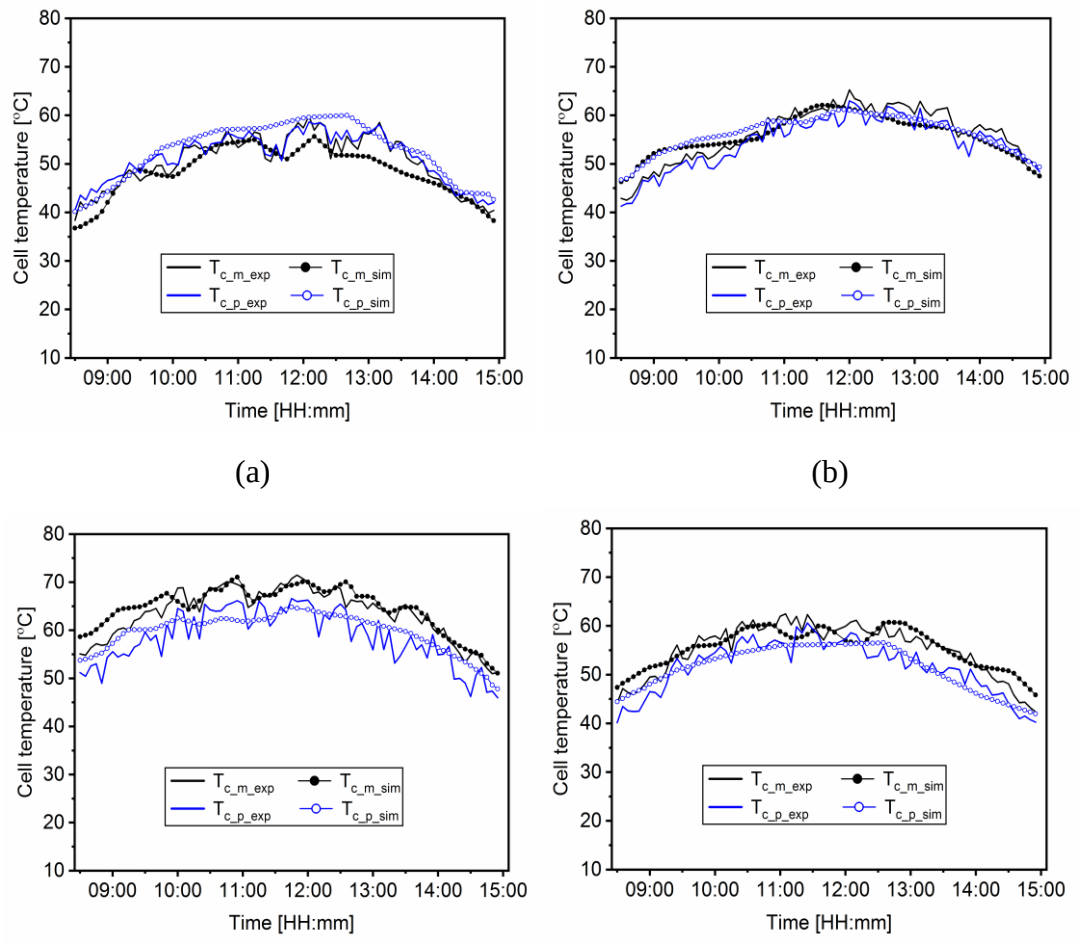

Figure 4.31 Validation of the simulated cell temperature of PV modules with the experimental cell temperature for various seasons: (a) winter, (b) pre-monsoon, (c) SW monsoon, and (d) post-monsoon (subscript '*c*' for cell, '*m*' for m-Si, '*p*' for p-Si, '*sim*' for simulation and '*exp*' for experimental).

Table 4.14 Statistical errors of the developed thermal model in terms of T_c value for various seasons.

Season	p-Si				m-Si			
	MAE (°C)	MRE	RMSE (°C)	R^2	MAE (°C)	MRE	RMSE (°C)	R^2
Winter	2.0	0.04	2.5	0.88	2.4	0.05	3.1	0.83
Pre-monsoon	2.4	0.05	3.0	0.82	2.2	0.04	2.6	0.82
Monsoon	2.6	0.05	3.1	0.78	1.6	0.03	2.1	0.88
Post-monsoon	1.9	0.04	2.2	0.84	2.0	0.04	2.4	0.84

4.3.3 Validation of the electrical model

The *I-V* and *P-V* characteristics of a PV module obtained from the developed model (section 3.1.3) are validated using the experimental results shown in Figure 4.32. This characteristic is obtained at instant of time of the day with G_{sim} and G_{exp} values of 707.62 W/m^2 and 765.04 W/m^2, respectively. The relative error in I_{sc} and V_{oc} values are 0.08 and 0.03, respectively. The relative error in P_{max} is 0.05. It is observed that the I-V and P-V curves have quite similar trends. However, a deviation in the curves could be seen, and this is due to the difference in values of the spectral irradiance, series and shunt resistances obtained from the simulation and experimental campaign.

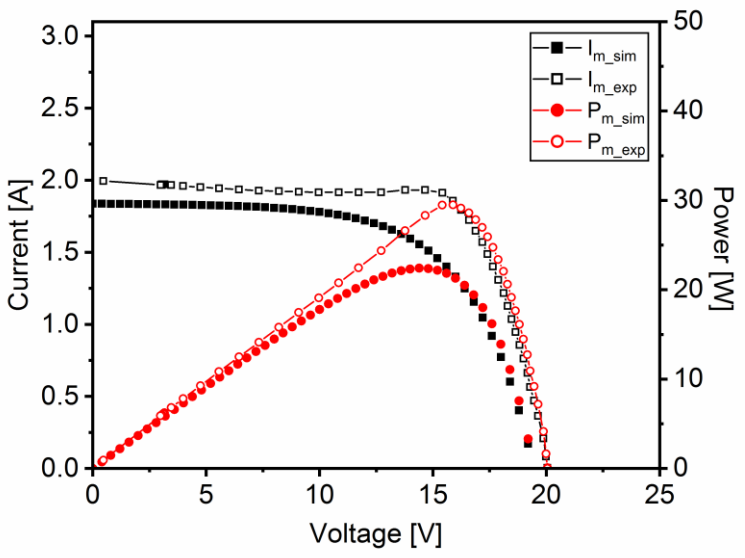

Figure 4.32 Validation of the *I-V* and *P-V* curves of a m-Si PV module.

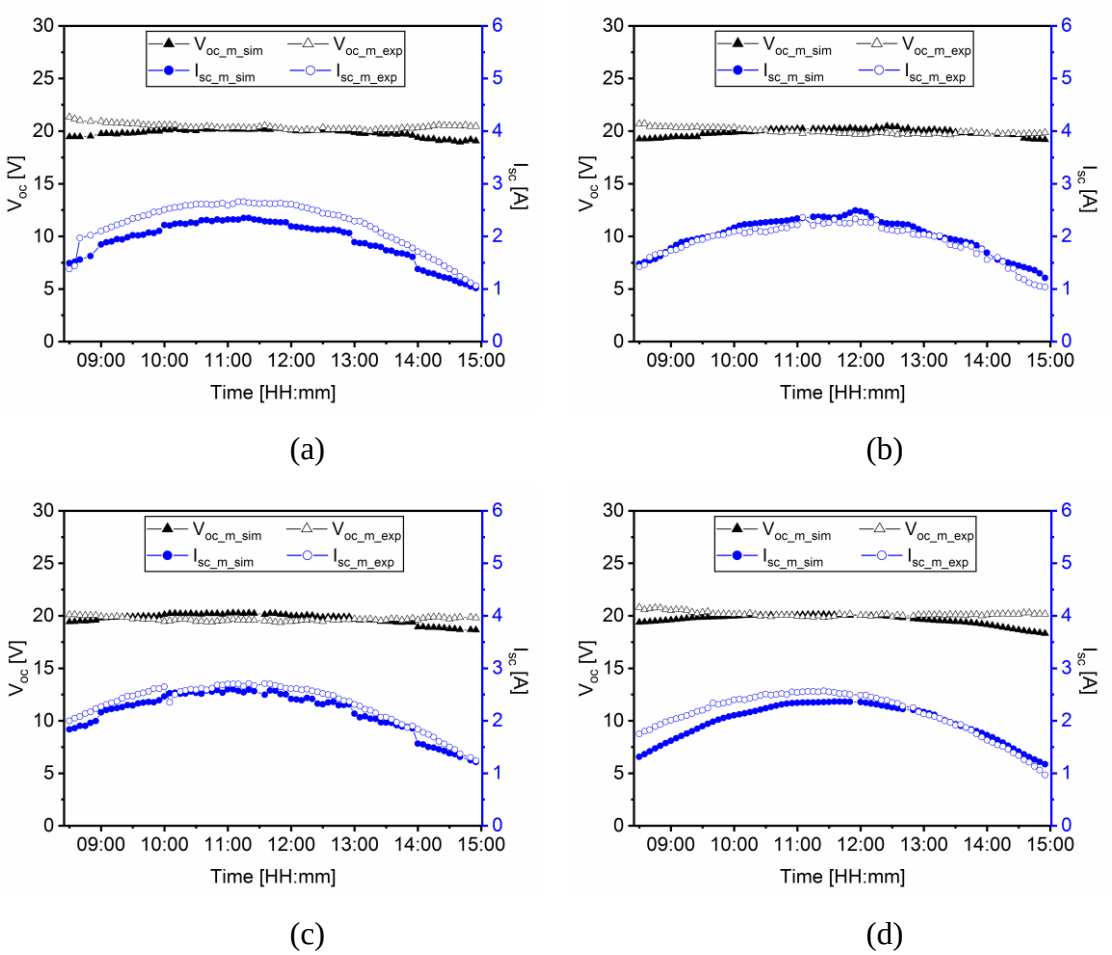

Figure 4.33 The experimental and simulated I_{sc} and V_{oc} values of m-Si for (a) winter, (b) pre-monsoon, (c) SW monsoon, and (d) post-monsoon days.

Figure 4.33(a)-(d) shows the comparative plot of the experimental and simulated I_{sc} calculated using equation (3.24) and V_{oc} using equation (3.30) values of the m-Si for various seasons of the year. The p-Si showed a similar trend for the mentioned parameters. During the winter, the measured I_{sc} value for m-Si and p-Si ranges from 1.1-2.7 A and 0.6-2.7 A, respectively. The measured V_{oc} value ranges from 20.0-21.4 V for m-Si and 19.7-21.1 V for p-Si. During the pre-monsoon, the range of the measured I_{sc} value for m-Si and p-Si are 0.3-2.4 A and 0.4-2.5 A, respectively; the measured V_{oc} value ranges from 19.0-20.8 V for m-Si and 19-20.4 V for p-Si. For the SW monsoon day, the measured I_{sc} value for m-Si and p-Si ranges from 0.8-2.7 A and 0.7-2.8 A, respectively; the measured V_{oc} value ranges from 19.4-20.4 V for m-Si and 19.4-20.2 V for p-Si. The measured I_{sc} value for both m-Si and p-Si during the post-monsoon day ranges from 0.6-2.6 A, and the measured V_{oc} ranges from 19.9-21.0 V for

m-Si and 19.6-20.7 V for p-Si. The statistical error MAE, MRE, and RMSE values of I_{sc} and V_{oc} for both m-Si and p-Si are shown in Tables 4.15 and 4.16, respectively. Therefore, the results showed a very small RMSE value for both the considered PV technology. The higher difference in the V_{oc} value may be due to the deviation in the simulated T_c of the PV module.

Table 4.15 Statistical errors of the I_{sc} and V_{oc} values of the m-Si PV module.

Season	m-Si					
	I_{sc}			V_{oc}		
	MAE (A)	MRE	RMSE (A)	MAE (V)	MRE	RMSE (V)
Winter	0.29	0.13	0.31	0.58	0.03	0.77
Pre-monsoon	0.10	0.06	0.12	0.41	0.02	0.53
SW monsoon	0.14	0.06	0.15	0.50	0.03	0.59
Post-monsoon	0.17	0.08	0.17	0.57	0.03	0.78

Table 4.16 Statistical errors of the I_{sc} and V_{oc} values of the p-Si PV module.

Season	p-Si					
	I_{sc}			V_{oc}		
	MAE (A)	MRE	RMSE (A)	MAE (V)	MRE	RMSE (V)
Winter	0.43	0.19	0.43	0.52	0.03	0.68
Pre-monsoon	0.13	0.07	0.16	0.39	0.02	0.48
SW monsoon	0.29	0.12	0.30	0.46	0.02	0.53
Post-monsoon	0.29	0.14	0.29	0.47	0.02	0.63

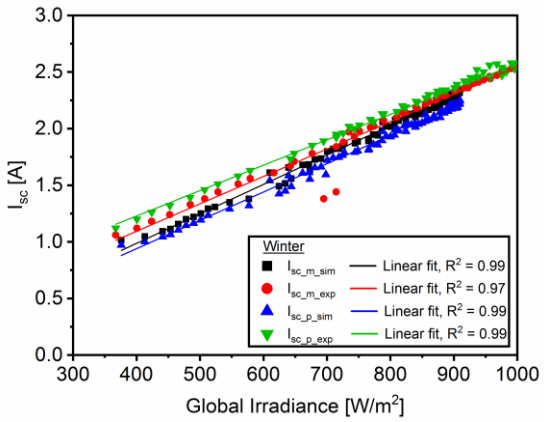

(a)

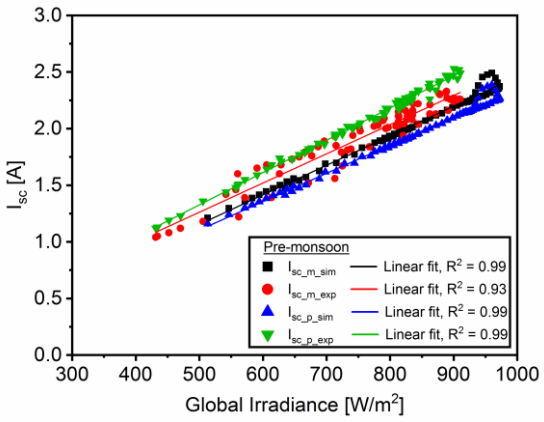

(b)

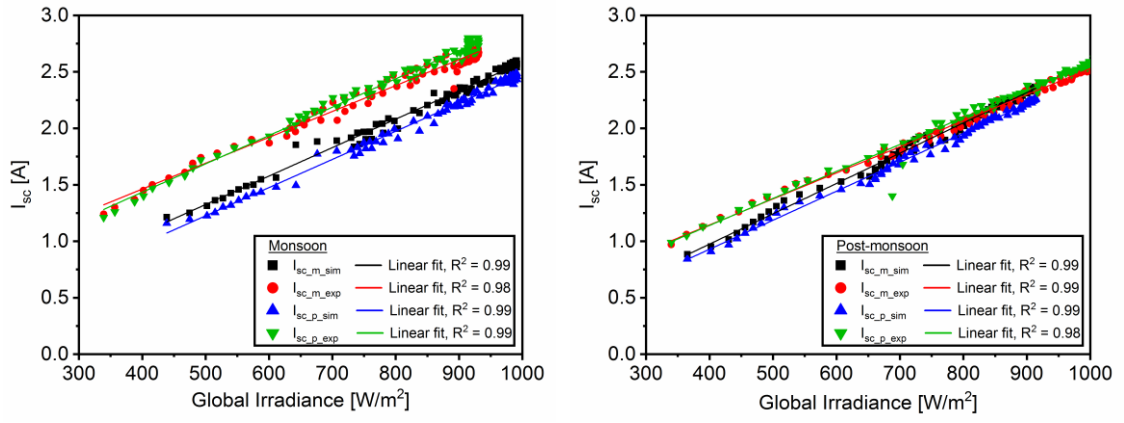

(c) (d)

Figure 4.34 The linear fit between the short-circuit current (I_{sc}) and global irradiance (G) during various seasons for m-Si and p-Si.

Figure 4.34 shows the variation of the I_{sc} with the global irradiance (G) for both the simulation and experimental data set along with their linear fit. It is observed that the I_{sc} varies linearly with G and for various seasons the R^2 value is above 0.9. The slope of the linear fit between the I_{sc} and G is found to be similar.

The P_{max} obtained for the model has been validated with experimentally measured data for various seasons, as shown in Figure 4.35 to Figure 4.38. Figures 4.35(b), 4.36(b), 4.37(b) and 4.38(b) show the relation between the P_{max} and global irradiance (G) for both simulation and experimental data set. A linear correlation with R^2 above 0.97 is obtained for all seasons. It is observed that as G increases, P_{max} increases. The slope of the linear fit for simulated dataset is 0.04 and 0.03 for experimental dataset. It is observed that at higher G, the simulated P_{max} is higher than the experimental P_{max}. This difference in slope may be due to the difference in the V_{oc} value (as shown in Figure 4.33). For higher value of G, the simulated V_{oc} is higher than the experimental V_{oc} and for lower value of G; the simulated V_{oc} is lower than the experimental V_{oc}. The reason to such difference may be due to the temperature variations in the developed model.

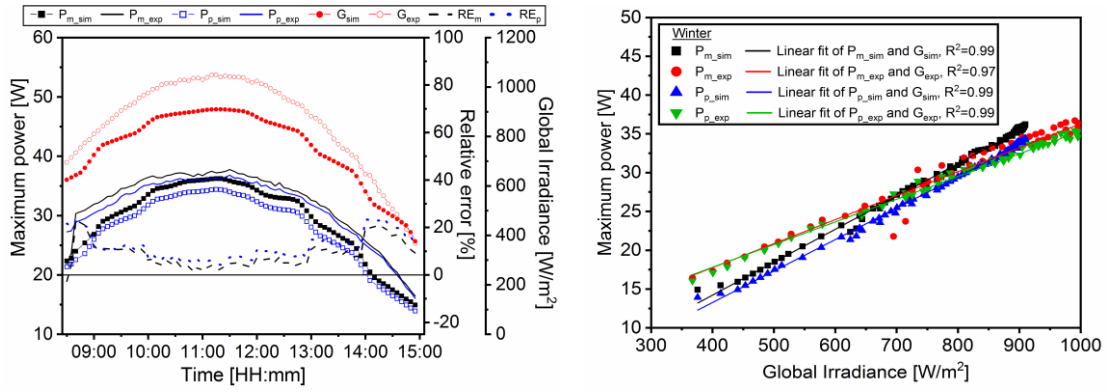

(a) (b)

Figure 4.35 (a) Comparison of simulated and experimental P_{max} and (b) linear fit between the maximum power and global irradiance, during winter season. RE is the relative error.

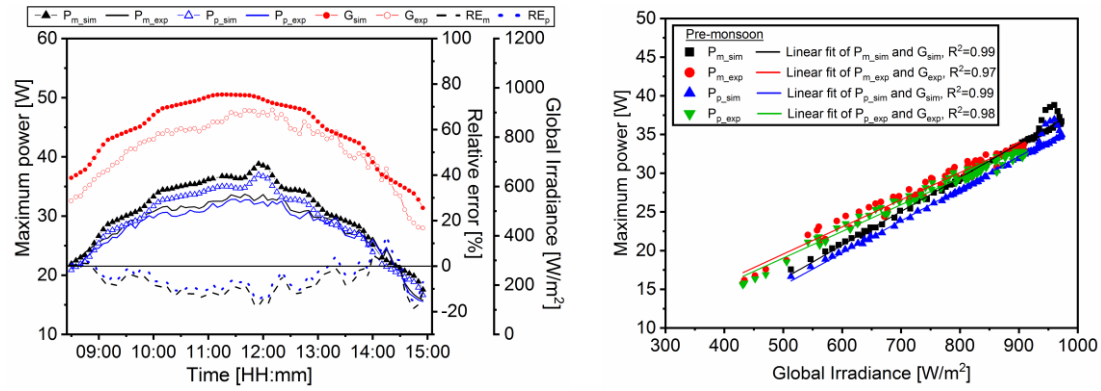

(a) (b)

Figure 4.36 (a) Comparison of simulated and experimental P_{max} and (b) linear fit between the maximum power and global irradiance, during pre-monsoon season. RE is the relative error.

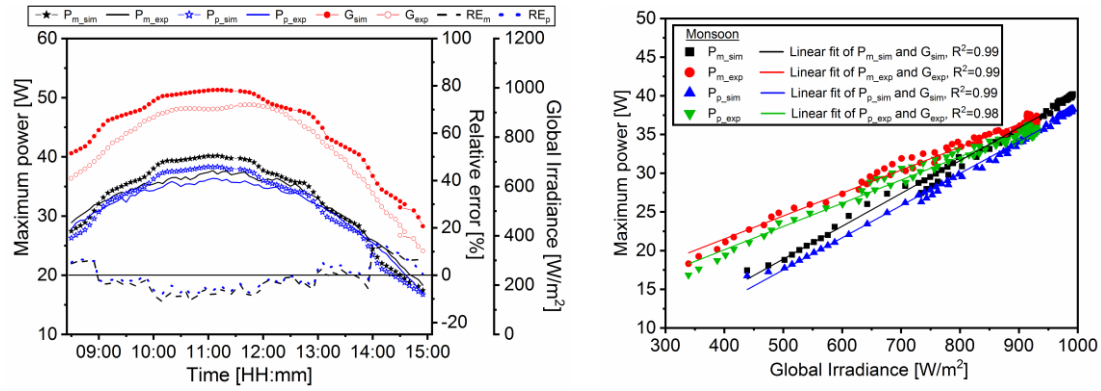

(a) (b)

Figure 4.37 (a) Comparison of simulated and experimental P_{max} and (b) linear fit between the maximum power and global irradiance, during SW monsoon season. RE is the relative error.

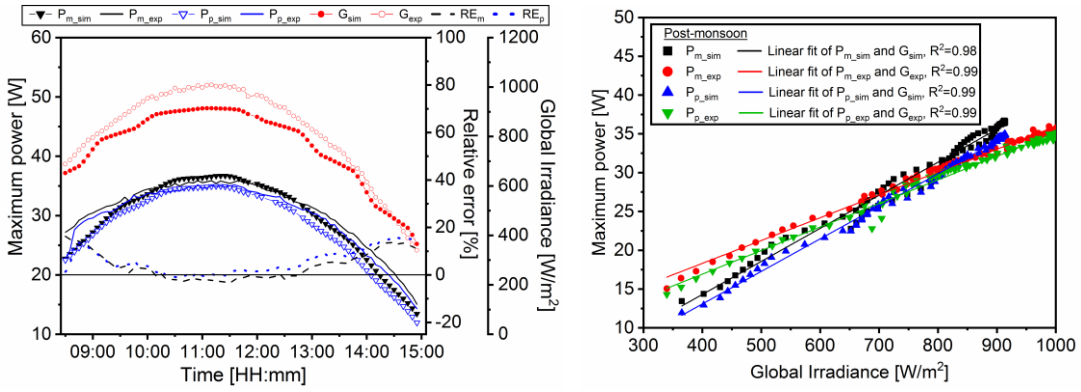

(a) (b)

Figure 4.38 (a) Comparison of simulated and experimental P_{max} and linear fit between the maximum power and global irradiance (right), for post-monsoon season. RE is the relative error.

Table 4.17 Statistical errors namely MAE, MRE, RMSE and R^2 of the P_{max} of p-Si and m-Si PV modules during various seasons.

Season	**p-Si**				**m-Si**			
	MAE (W)	**MRE**	**RMSE (W)**	**R^2**	**MAE (W)**	**MRE**	**RMSE (W)**	**R^2**
Winter	4.30	0.14	4.34	0.99	3.50	0.12	3.63	0.97
Pre-monsoon	2.06	0.07	2.30	0.94	2.88	0.10	3.16	0.93
SW Monsoon	1.15	0.04	1.41	0.99	1.19	0.04	1.41	0.99
Post-monsoon	2.32	0.09	2.46	0.98	2.04	0.08	2.34	0.99

The various statistical error and R^2 value is calculated for various seasons for both m-Si and p-Si and are tabulated in Table 4.17. The RMSE value of the P_{max} from the PV module for m-Si during winter, pre-monsoon, SW monsoon, and post-monsoon days are 2.92 W, 2.75 W, 2.02 W, and 1.83 W. For poly-Si, these values are found to be 3.63 W, 2.15 W, 1.70 W, and 1.88 W, respectively, which is better than one of the recent study [246]. The higher deviation could be seen during the morning and evening hours. The reason may be the spectral change and the variance in voltage value. The deviations in the predicted values may be due to the error in the predicted T_c of the PV module, which affects the predicted P_{max} of the PV module. Moreover, there exist some experimental errors, such as set-up uncertainties, transmission line losses, and time lag while recording real-time data [246]. Overall, the simulated P_{max} showed a good match with the experimental P_{max} value. The percentage difference between the simulated and

experimental values is also plotted for various seasons (Figure 4.35), exhibiting that the relative error range is quite acceptable [246].

Table 4.18 Comparative analysis of statistical error (RMSE) of PV module parameters with previously reported models.

Model	Season	I_{sc} (A)	V_{oc} (V)	P_{max} (W)	T_c (°C)
Yaman et al. [246]	Winter	0.23	1.34	5.09	1.34
	Summer	0.17	0.78	3.91	1.29
Jha et al. [137]	Summer	-	-	-	1.05
King et al. [161]	Winter	-	-	-	2.22
	Summer	-	-	-	3.78
Duffie et al. [222]	Winter	-	-	-	2.76
	Summer	-	-	-	4.73
Present	Winter	0.43	0.68	3.63	2.03
	Summer (SW Monsoon)	0.30	0.53	1.70	2.15

A comparative table between the existing models and the present model considering the statistical error (RMSE) of the parameters such as I_{sc}, V_{oc}, P_{max}, and T_c has been summarized in Table 4.18. Though considering the RMSE of I_{sc}, the present model exhibits a slightly higher RMSE. However, the RMSE of the V_{oc} and P_{max} is comparatively low in the present model. Moreover, the RMSE of T_c is lower than some of the reported work [161, 222] and higher than the other cases [137, 246]. It is observed that the present model can predict the thermal and electrical characteristics of the PV module at transient conditions under the influence of varying solar spectrum and environmental parameters with better accuracy and minimal involvement of complex equations, considering the most important parameters such as V_{oc}, and P_{max} and in some cases T_c also.

4.4 Analysis of energy yield using developed model and soiling effect

The energy yield from both the m-Si and p-Si PV modules is evaluated for the representative clear sky day of various seasons, as shown in Figure 4.39. Among the seasons, the highest energy yield is obtained during the summer season; this is attributed to the higher spectral intensity during the season. The percentage change in the simulated energy yield compared to the experimental energy yield is depicted in

Table 4.19. The deviation between the simulation and experimental typical energy yield is in the range of 2.40-8.06% and 1.10-10.9% for m-Si and p-Si, respectively.

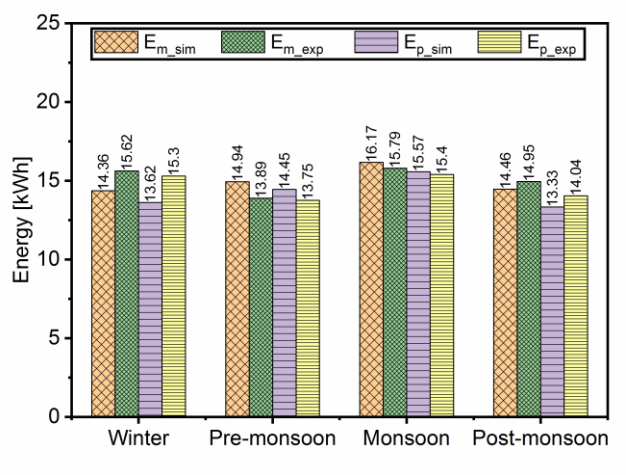

Figure 4.39 Validation of the energy yield obtained from the m-Si and p-Si PV modules for various seasons.

Table 4.19 The percentage change in simulated energy yield in comparison to experimental energy yield for m-Si and p-Si under varying seasons.

Seasons	**Percentage change in energy yield (%)**	
	m-Si	**p-Si**
Winter	8.06	10.98
Pre-monsoon	7.55	5.09
SW monsoon	2.40	1.10
Post-monsoon	3.27	5.05

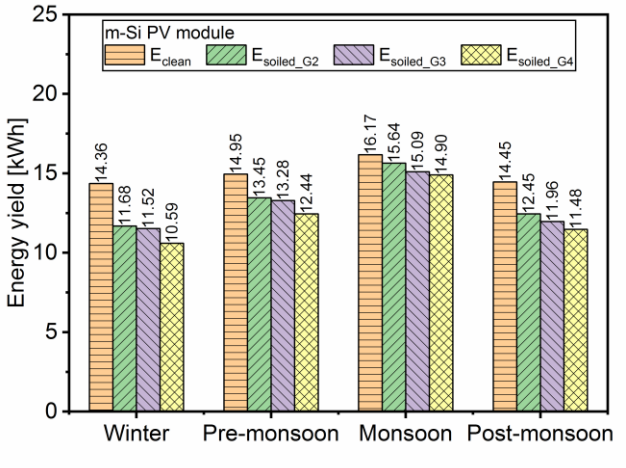

Figure 4.40 Typical **e**nergy yield of m-Si PV module under clean and soiled conditions for cleaning cycles (weekly: G2, monthly: G3, and never cleaned: G4, as described in section 4.2).

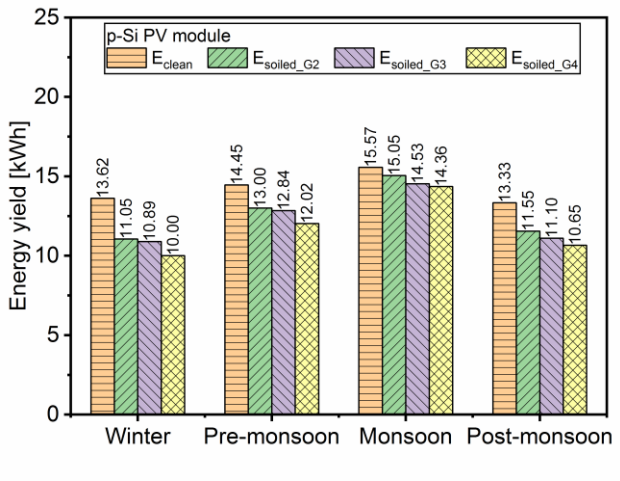

Figure 4.41 Energy yield of p-Si PV module under clean and soiled conditions for cleaning cycles (weekly: G2, monthly: G3, and never cleaned: G4, as described in section 4.2).

The seasonal energy yield is also evaluated for soiled conditions for both m-Si and p-Si PV modules. This is obtained using equation (3.41), considering the average relative transmittance of the glass coupons for a particular season (as described in section 4.2.1). The evaluation of the energy yield is done for the PV modules under weekly cleaned (G2), monthly cleaned (G3), and never cleaned (G4) conditions. The typical energy yield obtained from the clean and soiled conditions is presented in Figures 4.40 and 4.41, for m-Si and p-Si PV modules, respectively.

Table 4.20 Percentage deviation in the energy yield of the m-Si and p-Si under soiled conditions (different cleaned cycles) compared to clean conditions for various seasons.

Seasons	**Percentage change in energy yield (%) due to soiling**					
	m-Si			**p-Si**		
	Weekly cleaned	**Monthly cleaned**	**Never cleaned**	**Weekly cleaned**	**Monthly cleaned**	**Never cleaned**
Winter	18.68	19.80	26.27	18.90	20.03	26.57
Pre-monsoon	9.98	11.10	16.76	9.98	11.11	16.78
SW monsoon	3.33	6.73	7.86	3.29	6.66	7.78
Post-monsoon	13.87	17.26	20.62	13.39	16.76	20.10

The percentage deviation in typical energy yield due to soiling compared to the clean condition for various seasons is provided in Table 4.20. The maximum reduction in energy yield of PV modules due to soiling is 26%, that is, during winter, followed by 20% during post-monsoon, then pre-monsoon with 16%, and the least during SW

monsoon with 7%. All these values are obtained when the glass surface of the PV modules (m-Si and p-Si) is left uncleaned.

4.5 Summary

In this chapter, the spectrum dependent electric-thermal model is developed. The electrical and thermal characteristics of the PV module is analysed to check its working as per the input variable and governing equations. The effect of soiling on the performance of PV module is investigated considering the seasonal variability. Here, the correlation between the soiling and the environmental parameters are determined. Based on the statistical F-test and t-test analysis of the transmittance of the glass coupons recommendations have been provided on the cleaning cycle required in warm temperate climate with a dry winter, hot summer and high humidity. The developed model is validated for various seasons using the experimental campaign and it is observed that the simulation results have a good match with the experimental results and the errors are within the acceptance level. The deviation in typical energy yield is in the range of 2.40-8.06% and 1.10-10.9% for m-Si and p-Si, respectively.